© Copyright by Ehsan Baseri 2016

All Rights Reserved

Evaluation of Implementing Thermoelectric Materials as a Power Generator

A Thesis

Presented to

the Faculty of the Department of Mechanical Engineering

University of Houston

In Partial Fulfillment

of the Requirements for the Degree

Master of Science

in Mechanical Engineering

by

Ehsan Baseri

May 2016

Evaluation of Implementing Thermoelectric Materials as a Power Generator

_____

Ehsan Baseri

Approved:

_____

Chair of the Committee
Dr. Philippe.J.Masson,
Assistant Professor
Mechanical Engineering Department

Committee Members:

_____

Dr. Anastassios Mavrokefalos,
Assistant Professor
Mechanical Engineering Department

_____

Dr. Eylem Tekin,
Associate Professor
Industrial Engineering Department

_____

Dr.Suresh K. Khator, Associate Dean,
Cullen College of Engineering

_____

Dr. Pradeep Sharma, M.D. Anderson
Chair Professor & Department Chair
Mechanical Engineering Department

Evaluation of Implementing Thermoelectric Materials as a Power Generator

An Abstract

of a Thesis

Presented to

the Faculty of the Department of Mechanical Engineering

University of Houston

In Partial Fulfillment

of the Requirements for the Degree

Master of Science

in Mechanical Engineering

by

Ehsan Baseri

May 2016

Abstract

The challenge of finding new energy sources or improving the efficiency of machines has become an important priority to scientists. A huge portion of provided energy becomes waste in the form of thermal energy. This fact sets the stage to look at recovering this wasted heat by Direct Heat-to-Electricity Conversion. Thermoelectric materials provide the opportunity to convert heat to electricity by thermoelectric generators (TEGs), which work under the Seebeck Effect. In this study, we focused on two less developed applications of TEGs. First, the feasibility of exciting High Temperature Superconductor coils by means of a TEG has been investigated. In this study, a physical model of the system in Simscape™/MATLAB has been prepared. Second, we focused on energy recovery from the waste heat source in cylindrical shaped equipment. An analytical approach has been served to offer the relation between geometrical variables or thermoelectric properties, and the maximum output power of Tubular Thermoelectric Generators (TTEGs).

Table of Contents

List of Figures

List of Tables

Chapter 1

1.1 Introduction

In today's modern world, the issue of increasing usage of energy has become an important one. The short period of using fossil energy in last 150 years, has set the stage for huge problems and even crises around the world for us. The main side effects of using fuel energy are the limitation of conventional sources of energy, which is resulted in political conflicts, and environmental and industrial issues. The Above-mentioned factors, along with the issue of global warming and CO2 emission, have excited and forced scientists to focus on this problem with extra effort. Global investment in this sector has been increasing strikingly. Official released data shows there were 257 billion dollars globally invested in renewable power and fuels in 2011(see *Figure 1).*

Scientists' effort in recent studies focused on two main areas. First is developing new systems with higher efficiency of desirable output with lower amount of waste energy. As we can see in *Figure 2,* a huge amount of generated energy national wide in U.S. became rejected waste energy after use. The 61 % waste energy in 2012 is traced. Effective steps should be taken to reduce this amount. To achieve this goal, industries have been spending a huge portion of their budget on new technical solutions to increase the efficiency of their products and reduce the percentage of rejected energy. For instance, automotive industries try to offer automobiles with high Mile per Gallon (MPG) to reduce the gas consumption. This course of action is taken by means of redesigning the products by removing sources of energy waste, implementing new

materials with desirable characteristics, and designing better. These systems can be created by considering optimization factors such as implementing fuel management, thermal management and other controlling feedback systems.

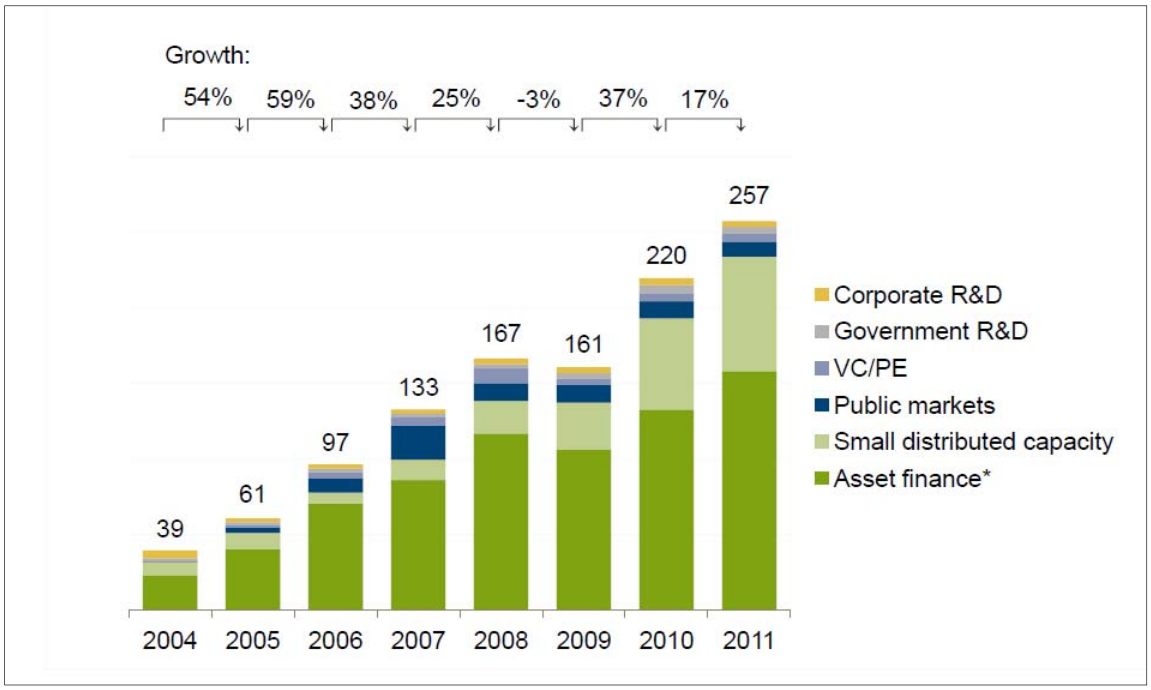

Figure 1. Allocated budget in billion dollars on renewable sources of energy from 2004 to 2011. [1]

Usually, inherent limitation such as the Carnot limitation for thermal motors, or friction energy of moving parts and scape of energy in form of heat, limits the efficiency, generates waste energy, and produces irreversibilities. Unfortunately, friction wastes the energy usually by producing low quality energy, which is not in most cases reasonable or feasible to recover by conventional methods. Any attempts to improve systems by reducing the source of irreversibility such as eliminating moving parts and recovering wasted energy would increase the efficiency of systems.

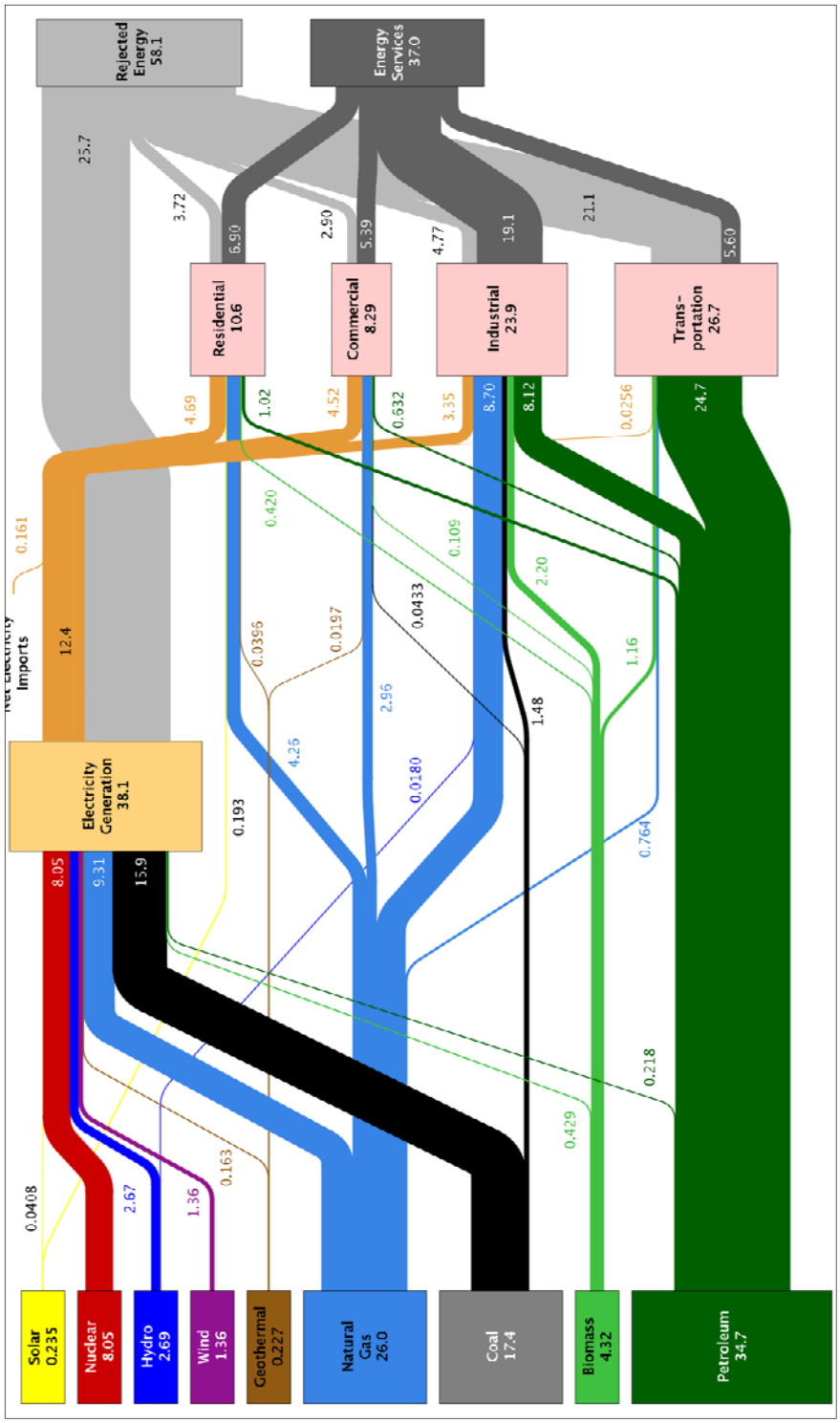

Figure 2.Huge amount of energy annually is rejected (61% in 2012) and sets stage for major problems. Technologies to recover this wasted energy are going to be critical for countries in next few years [2].Numbers in this chart are in quadrillion British Thermal Units

The second solution that has been studied by scientists is using new, renewable, and green sources of energy. The aim of this kind of development is to facilitate and provide enough energy for consumers by considering economic and environmental implications. Solar energy, geothermal energy, wind energy, wave energy, hydropower, and biomass are the new sources of energy with the most demand, and scientists and industries are focused on taking advantage of them. The main advantage of the renewable sources of energy is being environmentally friendly, sustainable, and accessible, as usually, at least one source is available in every area of the earth. The disadvantage of these new sources is that, these kinds of systems need more time and money to be developed from different aspects.

For example, in terms of levelized cost of electricity (LCOE), conventional sources of energy like coal and natural gas turbines cost less than solar energy. *Figure 3* LCOE is given by

$$LCOE = \frac{Cost\ over\ Life\ time}{Electrical\ energy\ over\ life\ time}. \qquad \text{eq. (1.1)}$$

These facts show that every tiny improvement in efficiency of implementing renewable sources of energy can make it more reasonable and attractive for industries to take advantage of them. By considering the above-mentioned factors, using thermoelectric generators (TEG) with its unique specifications would be an effective way to reach a higher performance of energy systems.

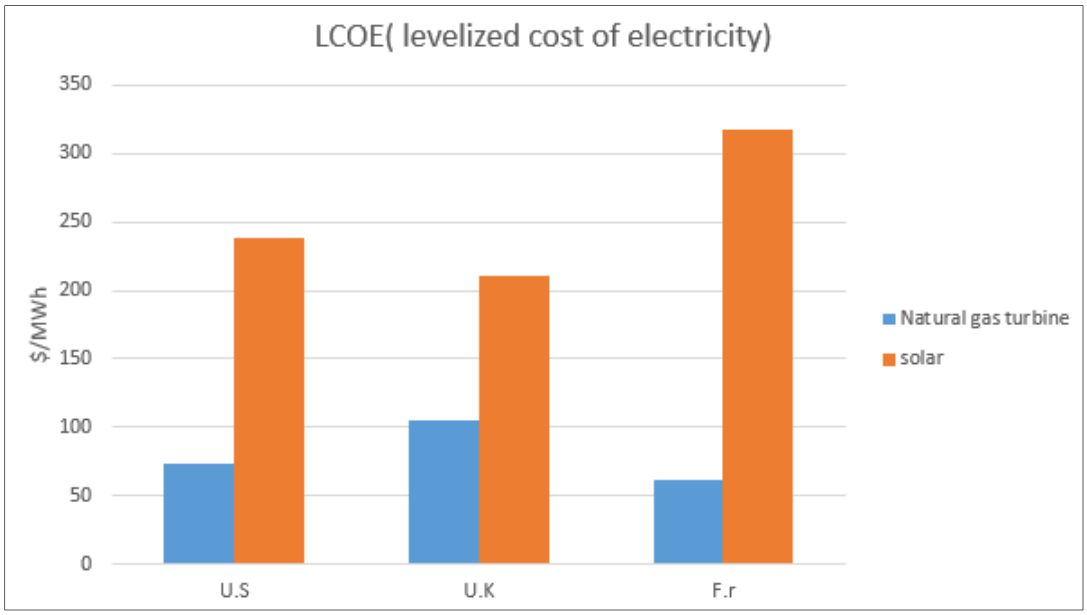

Figure 3 .Comparison of LCOE between solar source and natural gas turbine source in 3 developed countries. Generally, conventional sources of energy have less LCOE and it is huge obstacle for using renewable sources of energy. [3]

1.2 Motivation

The TEGs are categorized under the Direct Heat-to-Electricity Conversion systems. They have special characteristics such as working in a wide range of temperature, lack of moving parts, being noiseless, clean, having a long life, working permanently and easy implementation. The market of TEGs will be constantly growing from $40 M in 2014 to $940 M in 2024 [4]. TEGs can be used in systems with two purposes:

1- *Primary applications*: utilizing TEGs as a power source in order to feed a proportion of main system energy. This application of TEG is used in low power systems in remote areas, space applications that need a highly reliable source of energy or unpeopled zones or back up for other form of energy sources in case

of shut off the main source. The famous applications of TEGs Cathodic are protections of pipelines, unmanned radio transmitter sites, back up for solar photovoltaic panels and radioisotope thermoelectric generator in space explorations.

2- *Secondary applications*: utilizing TEGs as unit of recovering and harvesting waste energy in order to increase the efficiency of a system. This application of TEG is used along with other sources of energy to recover the main system's waste heat in order to increase energy efficiency, improve fuel economy or minimize the size of main source of energy in these systems. The famous application of TEGs in this field are automobile waste heat recovery from exhaust, plants' boilers and stacks heat recovery , and harvesting low frequency solar radiations energy.

Based on the application, selection between the higher power density and efficient conversion should be done. To minimize the size and mass of heat source, efficient conversion is important, and to achieve high electrical power and minimize the size of TEG, optimization on electrical power density should be done. We look at this concept in Chapter 3 more closely.

1.3 Concerns in Using TEG

Using TEG, as any other physical system has its own concerns, pros and cons. Field works and lab experiments confirm achieving more than 5% efficiency of TEGs are not feasible. Therefore, analyzing TEGs in different scales (materials, fabrication, and bulk design) should be carried out to achieve higher indices in energy management.

Maximizing “output power”, maximizing “efficiency” (or coefficient of performance), and reducing “cost per watt” of generated energy are the desirable indices, which scientists and industries are interested in. In this work, we study two different systems of energy with different concerns and approaches to using TEGs and feasibility of use.

In the first investigation, we look on TEGs in cryogenic temperatures and the usefulness of that in industrial or scientific purposes. We will answer the question of how much using of TEGs can be effective at a very low temperature to energize and stabilize the magnetic field in quasi-persistent High Temperature Superconductor(HTS) by providing a mathematical model and comparing it to previous experimental investigations.

In the second investigation, we analyze a special shape of TEGs, Tubular shaped TEGs, derive governing equations for ideal and realistic models, analyze these equations, find optimize design, and explain the effective variables on output power. We study the effectiveness and superiority of TTEG compared to flat rectangular TEG.

1.4 Principles of the Thermoelectric Effect

The Thermoelectric effect is a basic characteristic of conductors (a*lso*, semiconductors) which was discovered in 1800s. Experiments show that when two different materials connect in a point and heat the junction point, an electromotive force (EF) between the two open points will be generated (the Seebeck Effect). This procedure can be reversed by applying a voltage, creating a heat pump and making a

temperature difference (the Peltier Effect). Generated voltage is proportional to the temperature difference of the hot junction and the cold junction.

The proportion of generated voltage to temperature gradient is called the Seebeck Coefficient. Different types of materials can be used as a thermoelectric material.

1.4.1 Thermoelectric Generator:

The basic working principle of a thermoelectric generator is the Seebeck Effect. When we connect a point of two different conductors or semiconductors in a series and heat up the junction point, it generates a voltage differentiation between the two free points of the circuit. Generated electromotive force between two points is equal to $\Delta V = \alpha \Delta T$, which "$\alpha$" is a local Seebeck Coefficient with (V/K) or (μV /K) unit.

In *Figure 4*, when $T_A > T_B$, the positive α means the current direction is in a CW direction and negative α is in a CCW direction. [5] In other words, the temperature gradient and current direction indicated the sign of the Seebeck Coefficient.

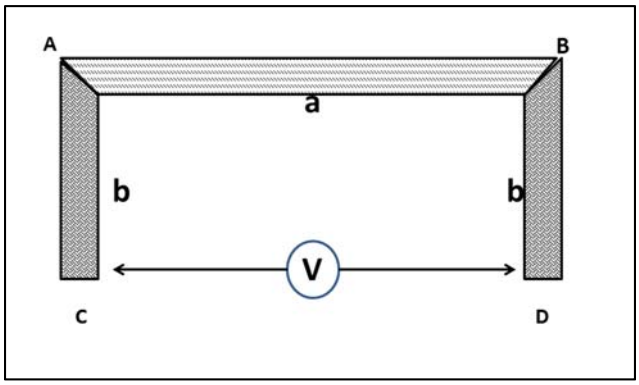

Figure 4 .Direction of current indicate the sign of Seebeck coefficient

Therefore, by making a series of materials with positive and negative S, higher accumulated voltage is achievable. By considering this improvement, manufacturers recently fabricated p-type n-type semiconductor TEGs. This kind of TEG consists of a p-type (with positive S) and an n-type (with negative S) semiconductor which is connected by highly conductive metal such as copper to connect in series electrically (*Figure 5*). Multisegmented or cascaded TEG that consists of different materials of TEG is offered as well (*Figure 6*). The idea behind the design of multisegmented TEG is that the greater Figure of Merit, the greater in energy conversion efficiency. However, the maximum Figure of Merit for every material occurs in specific range. Thus, because of the temperature gradient in thermoelements, especially in high gradient temperature difference, it is more reasonable to use materials in which their best Figure of Merit occurs in the temperature range of each segment. (*Figure 7*)

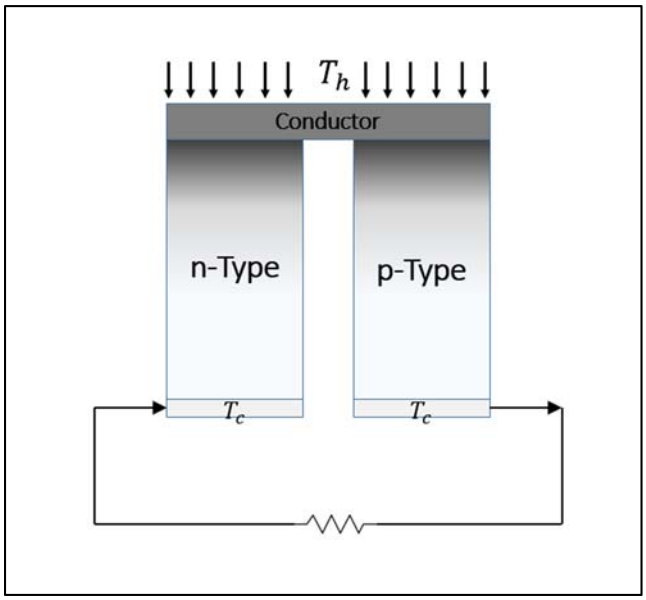

Figure 5. TEG consists of P-type N-type semiconductor legs

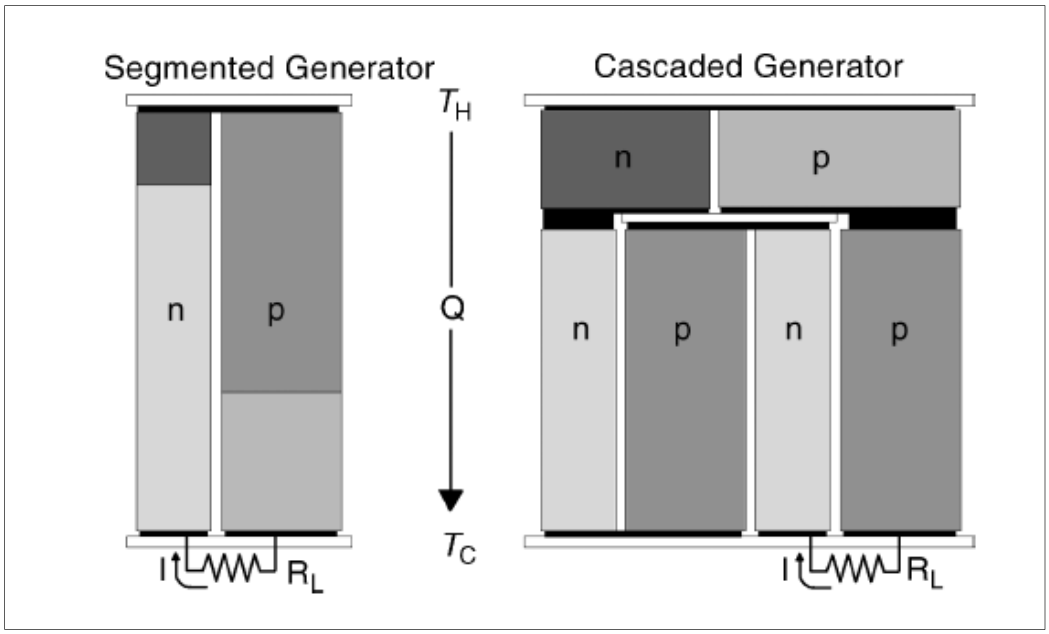

Figure 6. Schematic difference between segmented (Left) and cascaded (right). (From Ref. [6])

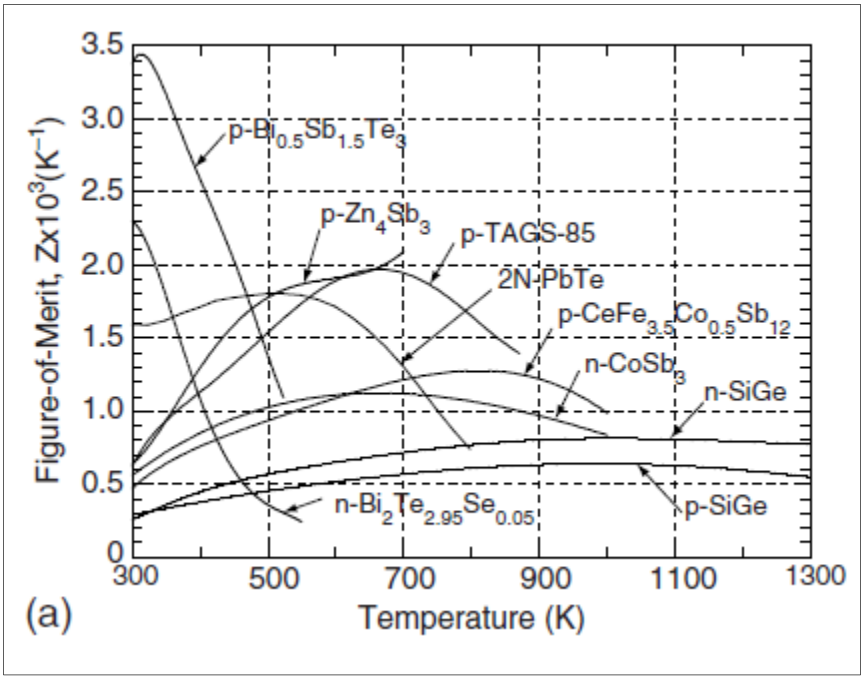

Figure 7. Shows dependency of Figure of Merit in some famous thermoelectric materials to temperature (Picture from Ref. [7])

1.4.2 Thermoelectric Materials:

As we will describe more in the following chapters, the thermoelectric properties of materials are measured in three quantities. These three include α, Seebeck Coefficient, σ(or $\frac{1}{\rho}$), the electrical conductivity, and k, the thermal conductivity. Figure of Merit is an index, which is defined based on these properties and given by

$$\mathrm{Z} = \alpha^2 \sigma/\mathrm{k}\,. \qquad \text{eq. (1.2)}$$

The relation between the efficiency of TEG and Figure of Merit is

$$\eta = \frac{(\mathrm{T_1} - \mathrm{T_2})\,(\mathrm{M}-1)}{\mathrm{T_1}\,(\mathrm{M} + {}^{\mathrm{T_2}}/_{\mathrm{T_1}})}\,, \qquad \text{eq. (1.3)}$$

where

$$\mathrm{M} = (1 + \mathrm{ZT_m})^{1/2}, \qquad \text{eq. (1.4)}$$

and $\mathrm{T_m}$ is an average of the hot junction and the cold junction temperatures. [8]

Increasing in $\mathrm{ZT_m}$ amount, results in increasing in the efficiency and for very large amount of Dimensionless Figure of Merit the efficiency approaches to $\frac{\mathrm{T_1} - \mathrm{T_2}}{\mathrm{T_1}}$ which the efficiency of Carnot Cycle. Therefore, Figure of Merit is an indicator of maximum efficiency of every thermoelectric material. Based on the above equation, bigger Seebeck Coefficient and electrical conductance, and smaller thermal conductivity are demanded to have higher efficiency. However, these properties are dependent, and

they are functions of free charge carriers' concentration. As we see in *Figure 7,* by increasing in carrier concentration, the Seebeck Coefficient is decreased, and electrical conductance and thermal conductivity are increased. Therefore, the maximum Figure of Merit occurs is tradeoff between these three properties that occurs in concentration of 10^{18} to 10^{21} carriers per cm^3 [9]. The bottom picture of *Figure 8* clearly shows that this carrier concentration has been in the semiconductor zone. Based on this fact, the higher performance thermoelectric materials are semiconductors. Some important and famous thermoelectric materials come in *Table 1*.

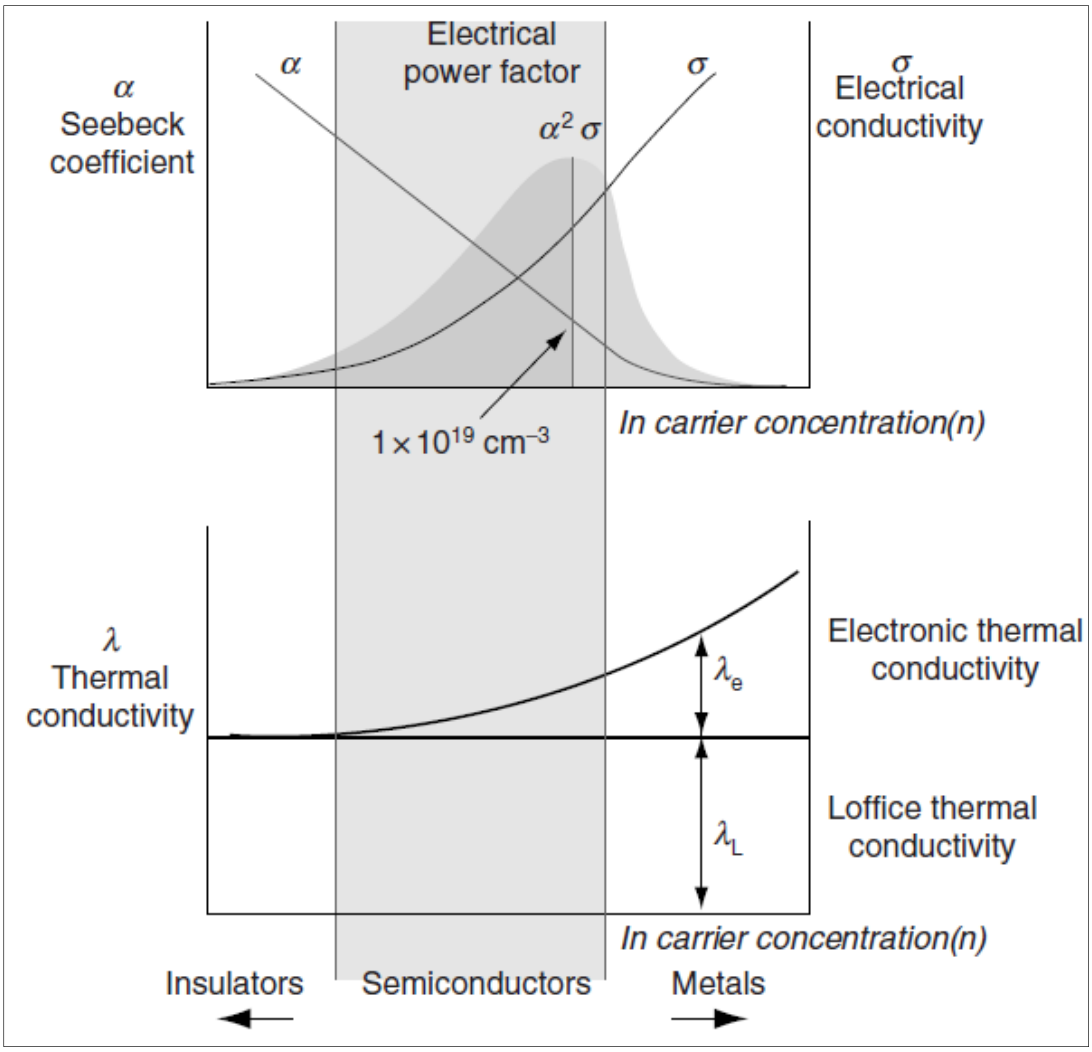

Figure 8. Thermoelectric properties are functions of carrier concentration. Power factor determines the capability of thermoelectric material to generate energy or move more heat (In Peltier Effect) that is equal to $\alpha\ \sigma^2$.Thermal conductivity is consisted of a constant amount λ_L (Loffice thermal conductivity) and a variable amount λ_e (Electronic thermal conductivity) (Figure from [5])

Table 1. Some famous materials for thermoelectric application. We have done our best to find the maximum achieved Figure of Merits reflect in this table.

Material	***Achieved ZT***
Bismuth and its nanostructures	Up to 2.4 in room temperature (300 K) for p-type $\mathbf{Bi_2Te_3/Sb_2Te_3}$ [10]
Graphene	Up to 3.21 at 600 k [11]
Lead telluride	Up to 2.2 at 915 K in p-type $\mathbf{PbTe}$ [12]
Silicon-germanium (SiGe)	Up to 0.7 at ~ 1000 K [13]
Solid solution of Magnesium and group IV compounds ($\boldsymbol{Mg_2B^{IV}}$) ($\boldsymbol{B^{IV}}$=Si, Ge, Sn)	Up to 1.68 at ~ 650 K for p-type $Mg_2Si_{0.6}Ge_{0.4}$ [14]
Sodium-Cobaltate	Up to 1 at 800 K for Na_xCoO_2 [15]
Tin Selenide	Up to 2.62 at 923 K [16]
Zinc Antimonide ($\boldsymbol{Zn_4Sb_3}$)	Up to 1.3 at 673 K [8]

Chapter 2

2.1 Introduction

Today's attitude to the sustainable form of energy sets a new stage for thermoelectric materials that can directly convert other forms of energy to electricity. Finding a proper way to consume or store this kind of energy with its unique characteristics (low voltage, high current, low power), requires precise selection among the vast variety of storage methods. Gould [17]studied a system that stored TEG energy in supercapacitors. Arrendale and Ahlbrandt [18]suggested using TEG to charge a superconducting magnet and store energy. Ono and Kuriama [19]set up an experiment that studied charging a superconducting coil by a TEG in the cryogenic temperature by means of temperature gradient which exist from outside to inside of HTS compartment. The latter case led us to study a reliable model of a coupled system of a Thermoelectric Generator (TEG) and a superconducting coil. Experiments have showed a generated high-Amp current is enough to keep the magnetic field stable in the quasi-persistent-mode HTS coil [19].

Previous works established mathematical modelling of TEG [20] [21]. A research group [22] developed a model based on analogy of thermal and electrical variables for thermoelectric cooler (TEC). This is a routine method for studying such a system provided in thermodynamics and heat transfer references [23] [24]. We use this model for TEG with some modification. Using MATLAB/SIMSCAPE to implement physical principles and mathematical equations is chosen to study characteristics, outputs, and

behavior of the system due to variables. At the end, we ran a simulation based on an experimental data and its assumptions, and compare the results of simulation and experiments together.

2.2 Principles and Physics of Superconductors

2.2.1 Superconductivity:

Superconductivity is a phenomenon in which the resistance of conductors becomes zero under a critical temperature. Heike Kamerlingh Onnes was the first to out the resistance of a wire of mercury abruptly became zero at 4.2 K. Further development in superconductor fabrication led to superconductors with critical temperatures of above 120 K. Superconductors with a critical temperature below 30 K are considered as Low Temperature Superconductors (LTS) and above 30 K are considered as High Temperature Superconductors (HTS). Recently, some scientists considered 77 K (boiling point of Nitrogen) as a split for LTS and HTS, because they can use liquid Nitrogen instead of liquid Helium to reach the critical temperature of HTS. Obviously, reaching 77 K is more feasible and inexpensive, so working with HTS is more desirable for engineers.

One of the most important model that describes superconductivity is the Critical State Model that demonstrates zero resistivity below critical current, as well as a jump in resistivity in that current. A more applicable model which is used more in an engineering application is the E-J power law that connect electrical field and current density by following power formula

$$E = E_c \left(\frac{J}{J_c}\right)^n, \qquad \text{eq. (2-1)}$$

where E is electrical field, and $\mathrm{J_c}$ is critical current density when $\mathrm{E_c}$= 1 μV/cm, and n is power which is function of field (B), temperature(T) and strain (ε).

By considering microscopic Ohm's law which states

$$E = \rho J . \qquad \text{eq. (2-2)}$$

we can define an equivalent resistivity for a superconductor and that will be

$$\rho_{sc} = \frac{E_C}{J_c} \left(\frac{J}{J_c\,(T_{sc})}\right)^{n-1} . \qquad \text{eq. (2-3)}$$

2.2.2 Superconducting coil:

Superconducting coil can efficiently store energy (up to 100% efficiency) with its unique characteristics such as a very low discharge time constant. Superconducting coil converts electrical energy to magnetic energy and stores it in the form of the magnetic field. According to Ampere law

$$\oint B \,.\, dl = \mu_0 \, I_{enc} , \qquad \text{eq. (2-4)}$$

where B is magnetic field (T), dl is the vector line element (m) with direction in the same sense as the current I. μ_0 is vacuum permeability ($\frac{H}{m}$), and finally $\mathrm{I_{enc}}$ is the current (Amp) enclosed by any arbitrary closed loop. Then the stored energy (E) is given by

$$E = \frac{1}{2} L I^2 , \qquad \text{eq. (2-5)}$$

where E is in Joule (j), L is inductance in henry (H) and I is current in Amp.

Therefore, these features set the stage for taking superconducting coil as a storage tool for the generated power of TEG. Low energy TEG is just implemented to excite HTS coil or use as power source to provide a persistent mode for non-persistent HTS coil [19]. HTS coil has a higher current decay than LTS coil due to higher flux flow creep in both exciting period and constant current period and need external power source [25]. Coupling a thermoelectric module and superconducting coil has assured the persistency of the magnetic field without an expensive and heavy external power source. Thus, considering the source of magnetic field decay in modelling should be investigated based on precision of the model, cost of simulation and behavioral dependency of the system on those variables.

2.2.3 Persistent Mode:

After the superconducting coil has been energized, it can be operated in the persistent mode by short-circuiting the coil's winding with a piece of a superconductor. When the windings become a closed superconducting loop, the power supply can be turned off, and currents will persist for months, yielding a very stable magnetic field. This is the advantage of persistent mode, which is not achievable with the best external power supplies. As a result, no energy is needed to power the windings [26].Therefore, by working in persistent mode; field decay should be below a certain level, typically 0.01

ppm in 60 minutes. However, in HTS magnets, it is very difficult to keep the magnetic field stable without a stable external power because an HTS coil has large flux flow resistance than a low temperature superconductor's coil. The magnet coil should take advantage from an external power source to keep the magnetic field stable. A superconducting magnet is a high current and low voltage system except for excitation voltage. Consequently, a thermoelectric generator unit is a very suitable power supply for a quasi-persistent mode magnet system [19].

2.3 Method and Model Building

2.3.1 Equivalence circuit:

Figure 8 describes the schematic physics of the system. HTS coil is simplified to a single coil with ideal conductance characteristics, two parallel resistors as superconductor resistivity ($\mathrm{r_{sc}}$) which has a nonlinear resistance behavior, and metal matrix resistivity ($\mathrm{r_{matrix}}$). The other sources of irreversibility are lead metal resistivity, internal resistivity of TEG element and an ideal power source.

Temperature difference between the hot side and the cold side of the TEG produces electromotive force and it excites the magnetic coil. We assume the cold side of the TEG is placed in a heat sink to remain in constant temperature (for example, it can fix inside the superconducting coil compartment with the constant temperature of 70 K), and a heater continuously raises the temperature on the hot side of the TEG.

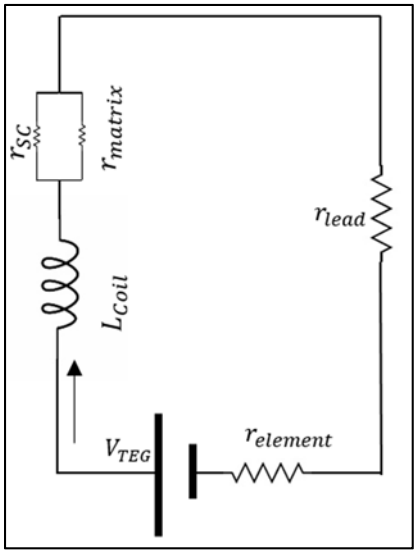

Figure 9. Overall schematic of TEG and HTS coil

In our model, we consider the empirical resistivity of the superconducting coil and the resistivity of the matrix in the simulation. Another method may be implemented to energize the coil. After connecting the TEG and the coil, reducing the temperature of the coil is started. It creates a temperature gradient in TEG and consequently provides an electromotive force.

2.3.2 TEG modeling

To find the generated voltage by total p-type n-type TEG, each semiconductor's leg is discretized to finite numbers of ΔX in the longitudinal direction. As long as we heat up just from one direction and the thickness is small enough, we can assume the heat transfer as a 1D thermal conduction in the legs. We consider each ΔX as a simple power source like a battery (*Figure 8*). The involved physical properties consists of:

$T: Temperature$

$r(T): Electric\ resistance$

$S(T): Seebeck\ Coefficient$

$K(T): Thermal\ conductivity$

All these properties are temperature dependent. For reducing computation cost and by considering some other involved factors we may neglect variation of properties due to temperature. Temperature domain, error percentage, and model precision are the main factors between which there should be tradeoff.

By discretizing the domain, we can easily adopt various material properties and other physical implementations.

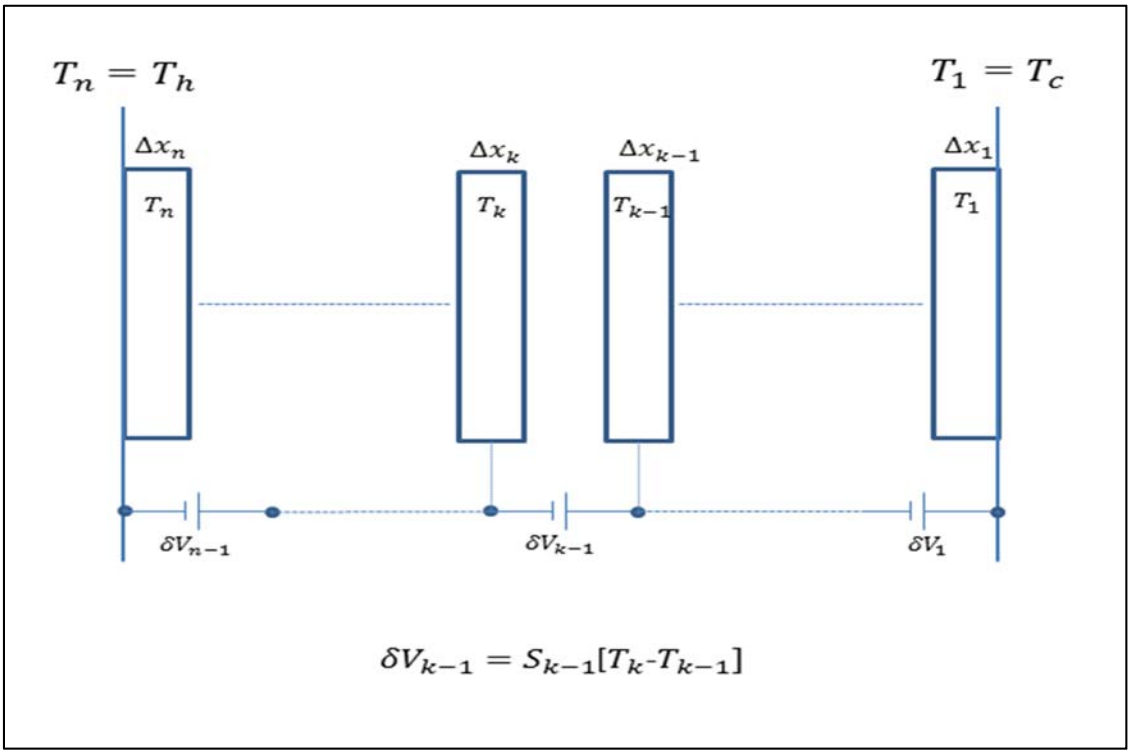

Figure 10. Schematic of discretizing a leg of TEG to n parts, between hot side and cold side of the leg.

n is the number of discretization, so the generated micro voltage of any arbitrary k-th element is given by

$$\delta V_{k-1} = S_{k-1}[T_k\text{-}T_{k-1}]\ . \qquad \text{eq. (2-6)}$$

Based on rules of accumulation of batteries in series circuits, the total accumulated voltage is given by

$$\Delta V = \sum_{n=1}^{n-1} \delta V_n\ . \qquad \text{eq. (2-7)}$$

All the above-mentioned steps can be abstracted to a simple flowchart in order to execute the model by computer. *Figure 11* shows the flow chart of this procedure.

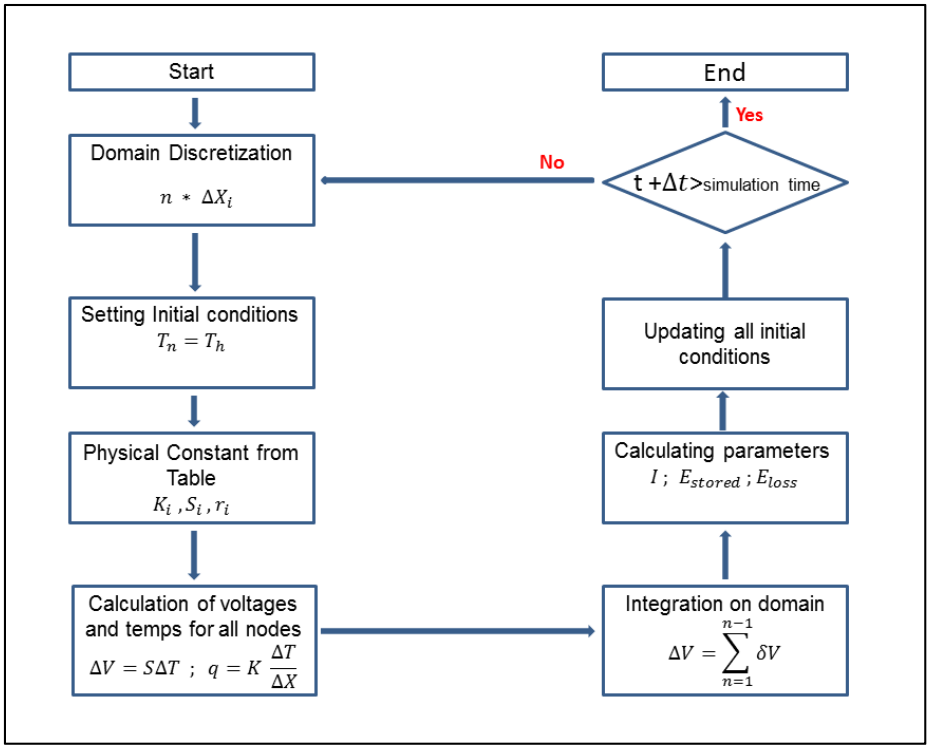

Figure 11. Flow-Chart of procedure

2.3.3 Coil and Other Load modelling:

At t=0, we assume boundary temperatures are the same ($T_h = T_c$) and by then, the heater increases the temperature in the hot side. In each time step, by considering initial conditions, temperature (T), thermal conductivity (K), Seebeck Coefficient (S) and electrical resistance of TEG are calculated. Consequently, because of the series configuration of the micro power source, by accumulation of micro voltages and gaining total EF, total current, inner resistivity of TEG and heat loss are calculated. As the time passes, the generated current will excite the coil and induce a magnetic field.

The electrical current of a closed circuit depends on summation of resistivity of external loads and internal resistance of the TEG. Total resistance can deduct to a superconducting coil with nonlinear resistivity (E-J relation), a parallel resistor (r_{matrix} and r_{SC}) and the other series resistor (r_{lead}) on behalf of lead metal resistivity plus the internal resistivity of the TEG. In other words:

$$\begin{cases} r_{element} = \rho \left(\frac{L}{A}\right)_{element} \\ r_{matrix} = \rho \left(\frac{L}{A}\right)_{matrix} \\ \rho_{sc} = \frac{E_C}{J_c} \left(\frac{J}{J_c\,(T_{sc})}\right)^{n-1}, \end{cases} \qquad \text{eq. (2-8)}$$

where E_c = 1 μV/cm (criterion for determination of J_c) , J is the current density, $J_c\ (T_{sc})$ is the critical current density, which is dependent on the temperature of the superconducting material; and n is the exponent, which varies for each transition stageand is measured by experiment. [27]

Then total resistance will be

$$R = r_{element} + \frac{r_{matrix}\, r_{SC}}{r_{matrix} + r_{SC}} + r_{lead} \qquad \text{eq. (2-9)}$$

and by considering Ohm's law and Seebeck effect we will have

$$\begin{cases} V = S\,\Delta T \\ V = R * I \end{cases} \quad \rightarrow \quad I = \frac{S\,\Delta T}{R} \qquad \text{eq. (2-10)}$$

in which I is the current of the circuit (and also coil) in Amp

2.4 Results

2.4.1 Simscape Modelling:

Based on the flowchart in *Figure 9*, we simulate our model in the MATLAB/SIMSCAPE. The main reason of selecting this library is that with Simscape, we can systematically create the model of physical systems within the Simulink environment. Simscape enables us to build our model systematically, based on physical interactions of inputs and variables. Every physical interaction demonstrates with blocks and connecting lines. Therefore, in each steps you can see the model visually and it reduces the effort to check and debug the model comparing to, let's say writing code. All numerical methods of solving systems of equations are provided in Simscape and we do not need to write a time-consuming code for our simulation. Besides, it enables us to make new blocks for those physical components, which have not been contrived in Simscape in advance. To take advantage of this ability of Simscape, knowledge of basic coding rules of MATLAB is needed. We utilize this ability

of Simscape to make new physical components. Schematic preview of simulation comes in *Figure 10.* Every block comes with its tag name. Rectangular blocks are physical elements, which consist of sub systems (*Figure 11* and *Figure 12*), and the other components are sensors (Voltage, current and temperature sensors) and graph plotters. The other specifications are coming in Table 2.

Table 2. Specifications of the HTS coil

Specifications of the HTS coil
Superconductor: Bi2223
Type: Single pancake coil
Inner diameter: 120 mm
Outer diameter: 300 mm
Height: 5.3 mm
Number of turns: 90

Two tables have been set in Simscape model, which consists of thermal conductivity and Seebeck Coefficient value as functions of temperature. In every time step, based on acquired temperature, these two properties (K and S) are extracted by interpolation. The relative data comes in *Table 3.*

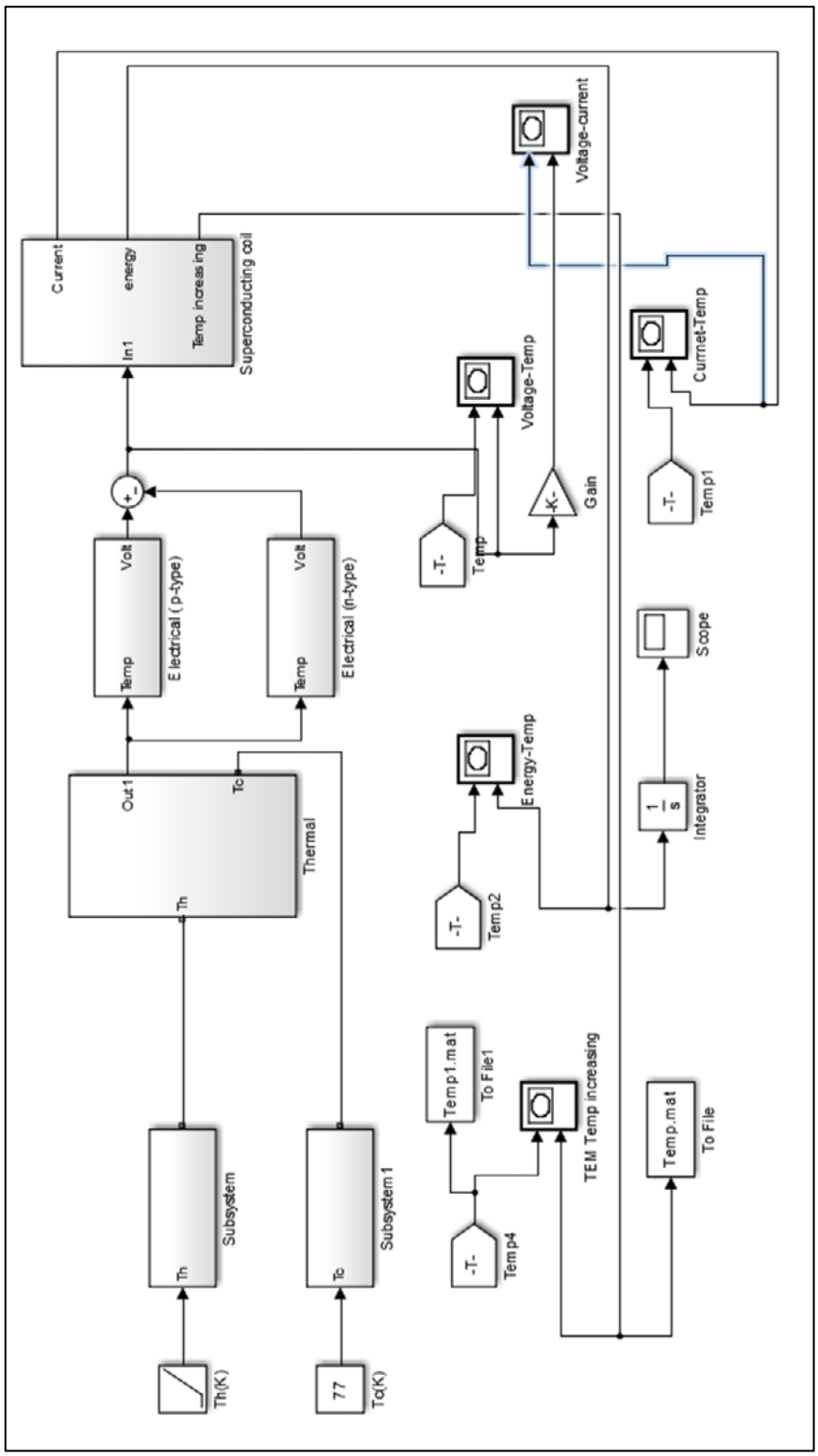

Figure 12. Screen shot of Simscape model. Shows the overall main components of system.

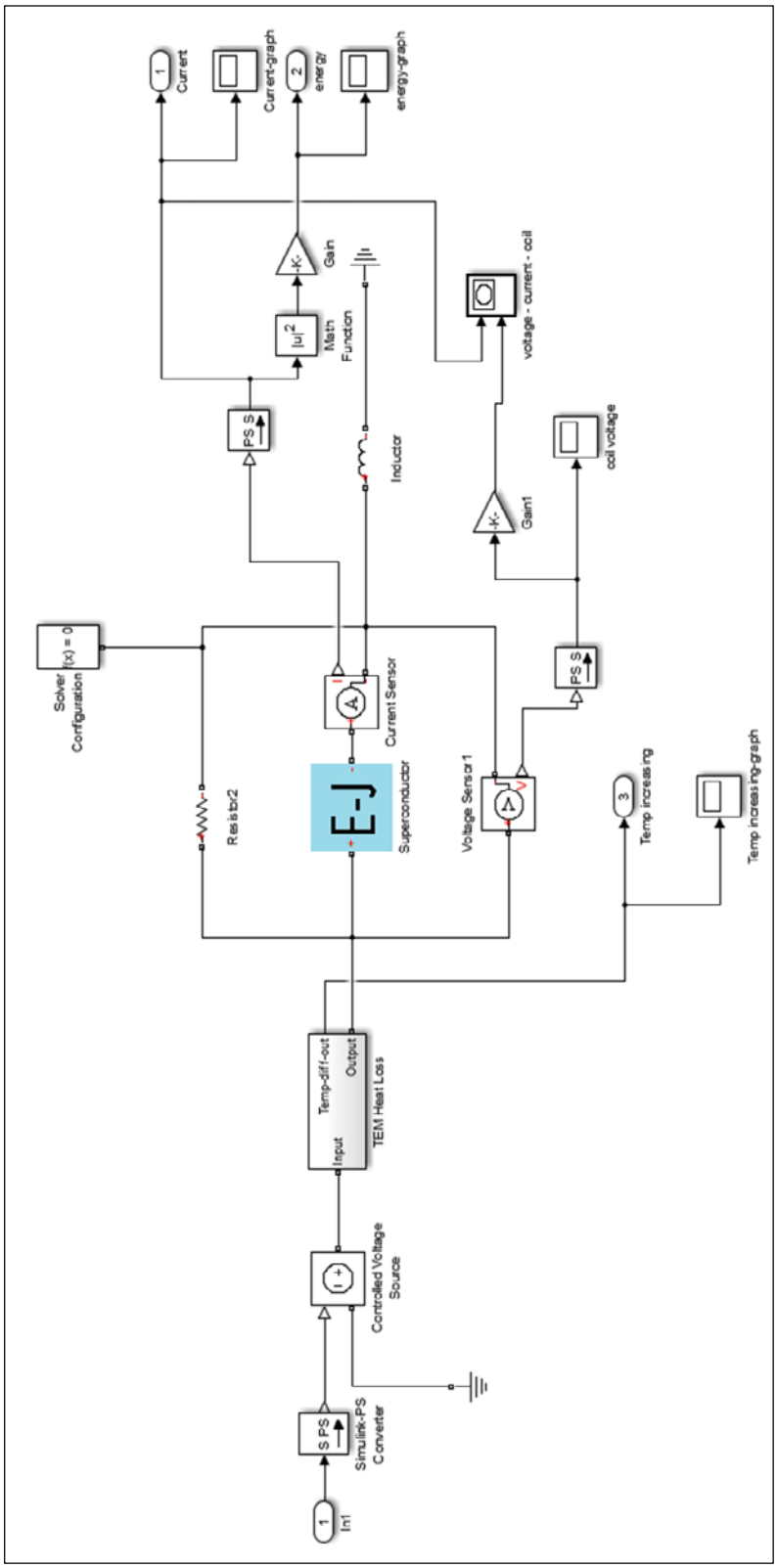

Figure 13. subsystem of superconducting coil

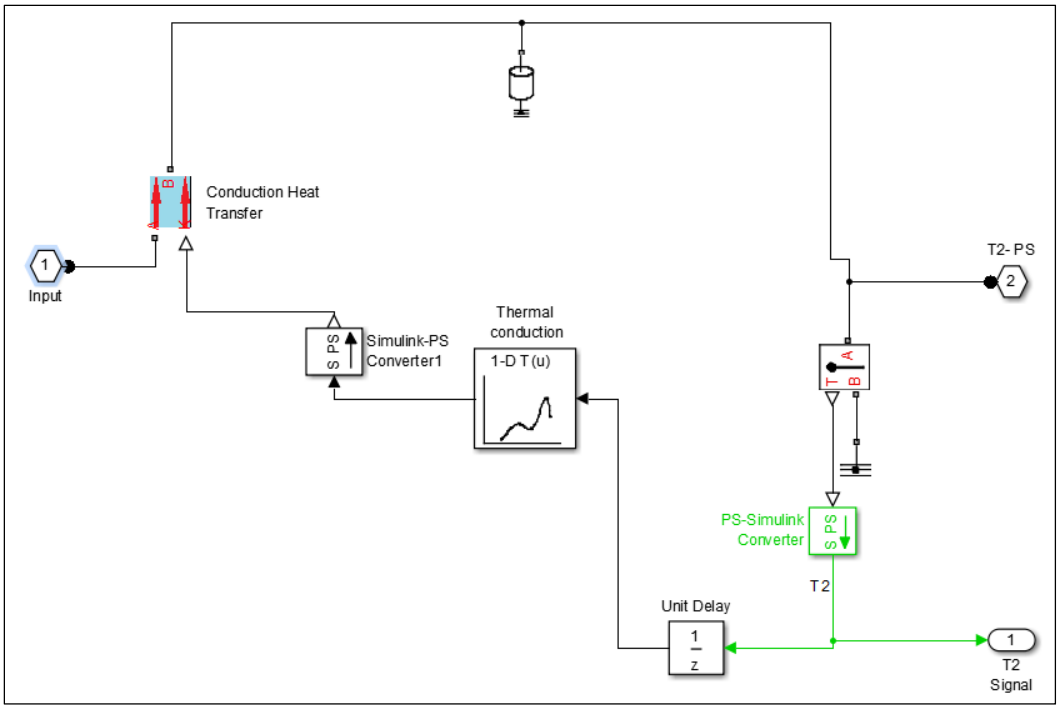

Figure 14. sub-block of one microelement of TEG.

Table 3. Seebeck Coefficient and thermal conductivity functions of temperature

$T\ (K)$	S (*10e-6) (V/K)	K (W/(m.K))
77	0	0
100	75	2.5
150	125	2
200	170	1.55

However, Simscape does not have default library for heat conduction with variable thermal conductance (K), or a library for superconductor resistivity. Therefore, we produced two new blocks in SIMSCAPE. The first is a thermal heat conductance block with variable K, which interpolates it from the external table in each time step. The other is a superconductor block, which simulates superconducting coil. Required input for this block comes in *Figure 15.*

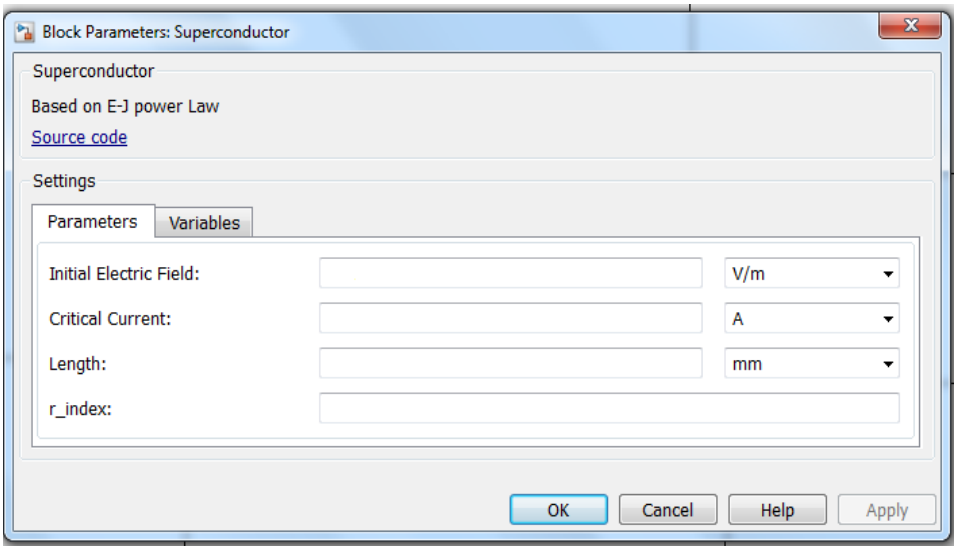

Figure 15. Customized block of superconductor coil in SIMSCAPE

2.4.3 Current and Stored Energy:

Figure 16 and 17 show the results of the simulation based on given assumptions and initial conditions of the experiment in reference [25]. The temperature of the hot junction is the only variable temperature, and it is demonstrated on the X-axis during

heating up by an external heater because the cold side is fixed in specific temperature and is constant (77 K, liquid Nitrogen temperature).

Figure 16 shows increasing trend of voltage with respect to temperature increasing, as expected. Experimental results and the results of our simulation in magnitudes and concavity of curves are highly compatible. An almost constant difference amount is seen between these two graphs. This difference may result from existing contact resistance between the TEG semiconductors and the copper conductor plate that connect two thermoelements. Considering this variable in the simulation needs a precise investigation of contact resistance.

In *Figure 17*, current growth versus temperature is seen. The results of the experiments and simulation are so compatible. In temperatures below 130 K, by very good precision, linearity is dominant. Above this temperature, a curvature occurs in the graph, which results from the exponentially trend of resistance and inductance in superconductor coil. Inductance is opposed to current growth, and after about 5-time constant ($T = \frac{L}{R}$), it acts like a simple resistor. This fact clearly expresses the curvature part of this graph.

Finally, the most important quantity comparison, the simulated and experimental relation between the input heat flux to the TEG and the transport current are shown in *Figure 18*. As we expected, increase of input heat results in higher current in the circuit. In this system, the generated heat in the heater becomes to the heat leakage in to the HTS coil.

Figure 19 illustrates the stored energy in the coil in different temperatures. Such a trend in stored energy is expected due to being the function of current squared, but there is not any experimental data to compare with.

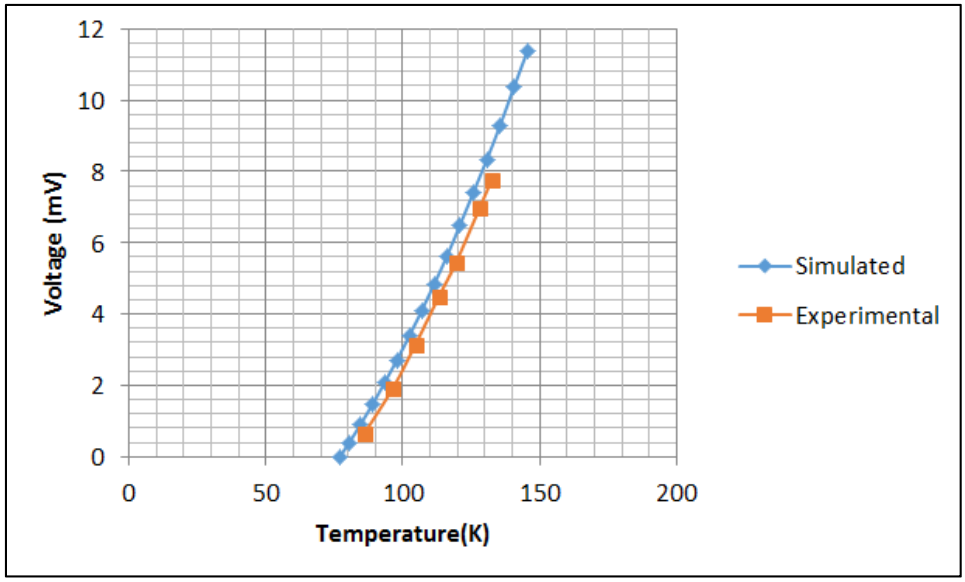

Figure 16. Voltage vs. Temperature

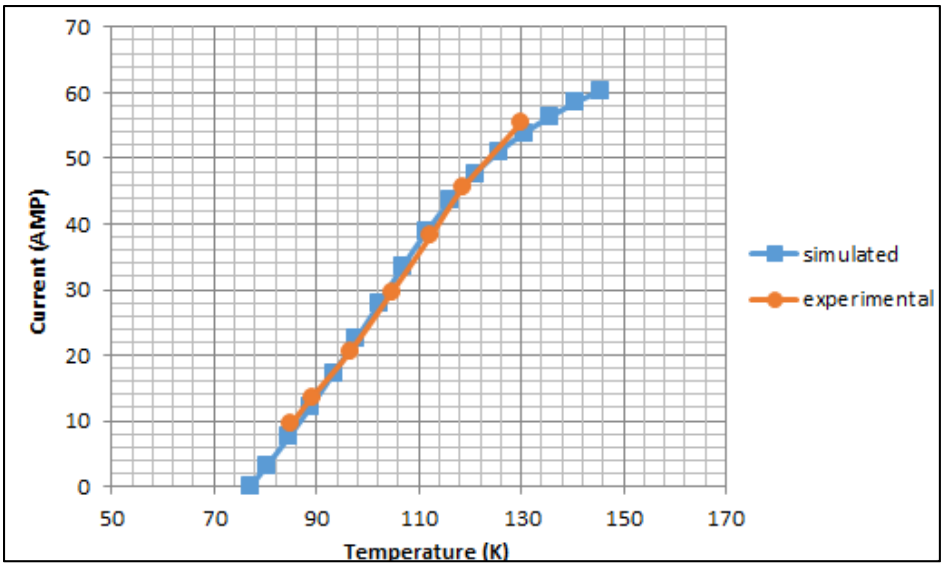

Figure 17. Current vs. Temperature

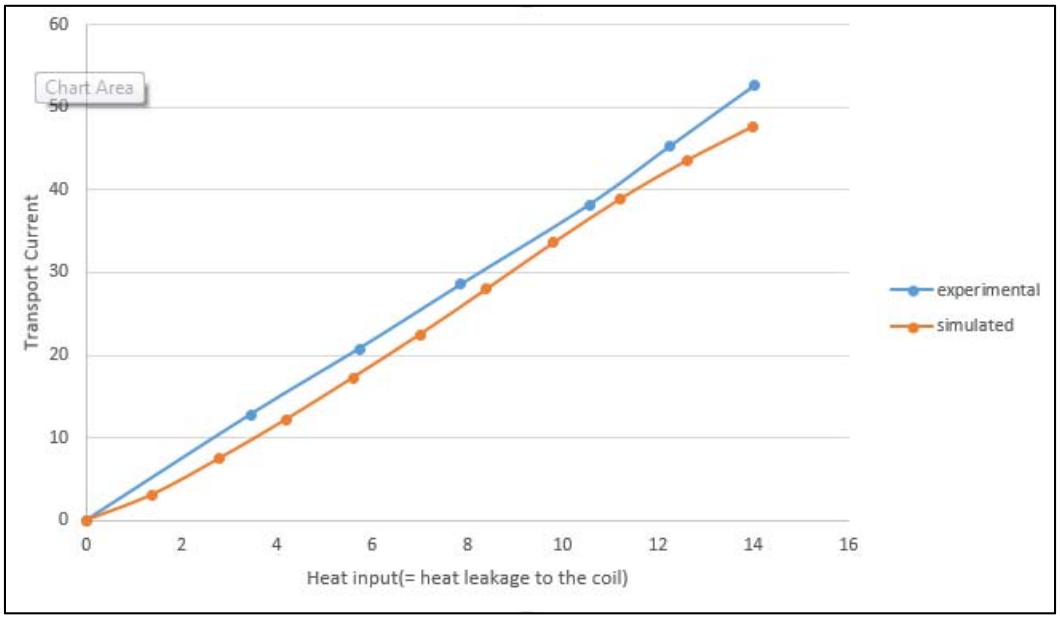

Figure 18. Current VS. Heat Input

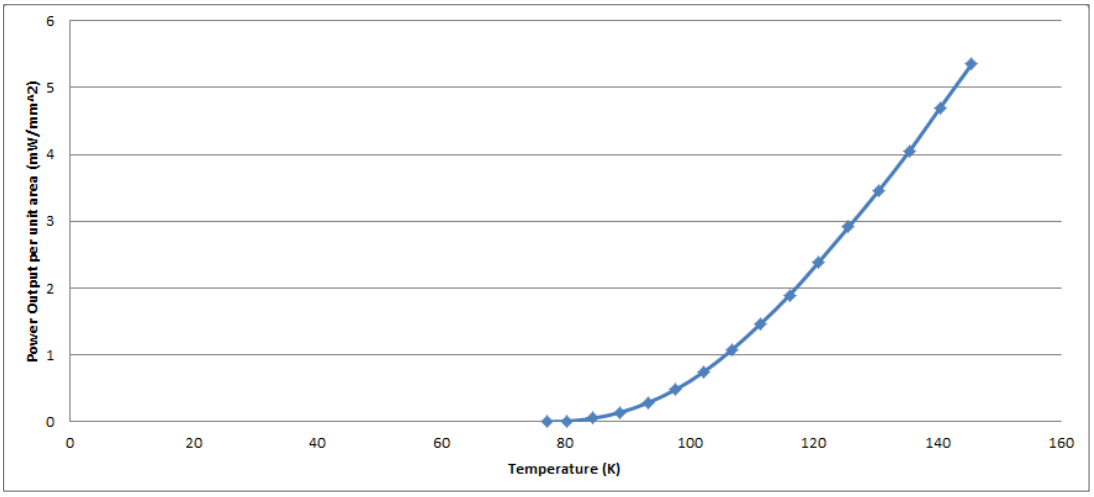

Figure 19. Stored energy in HTS coil when the TEG is heated up.

2.5 Conclusion

In the present work, our goal was to offer a general modelling that has the ability to cover a HTS coil that energize autonomously by a TEG when heating up the TEG or cooling down HTS coil. By considering generality, individuals may set simpler assumptions in their simulation, based on their computational potential and access to preliminary data.

Results in TEG model agree with the other experimental literature. Simulated model and experimental data in superconducting coil and electrical current are compatible in trend, behavior, and magnitude. MATLAB/Simscape by offering wide range of default electrical and mechanical elements (blocks) along with generating customize element (e.g., in present work making superconducting coil block), is a powerful tool to study such an interactive and multiphysics simulation.

In this work, just one individual unit of TEG is simulated. However, this model can be employed in the study of a farm of TEG units. This study is highly suggested to optimize the quantity, electrical and configuration of TEG units.

Chapter 3

3.1 Introduction

Some of the most important sources of wasting heat are in the shape of pipes and tubes. These tubes are good sources for harvesting energy because there are plenty of them in industrial plant or internal combustion engines (like automobiles), ventilation tubes and pipelines. Using a conventional rectangular TEG is not very wise for wrapping around a roundish surface such as pipes. Therefore, it is better to design tubular TEG that completely embraces the tube. The pioneer design is “US 4056406 A” patent in 1975 [28] (See *Figure 20).*

The design consists of two layers of inner and outer thermal conductor incorporating tubular shape p-type n-type thermoelements with interconnecting electric conductor strips. The insulation elements insulate the thermoelements from each other in order to avoid short circuit. To reduce energy loss in contact joints between the thermal conductors, electric insulation units and tubular thermoelements, the thermal conductors are crimped for producing pressing force acting on elements.

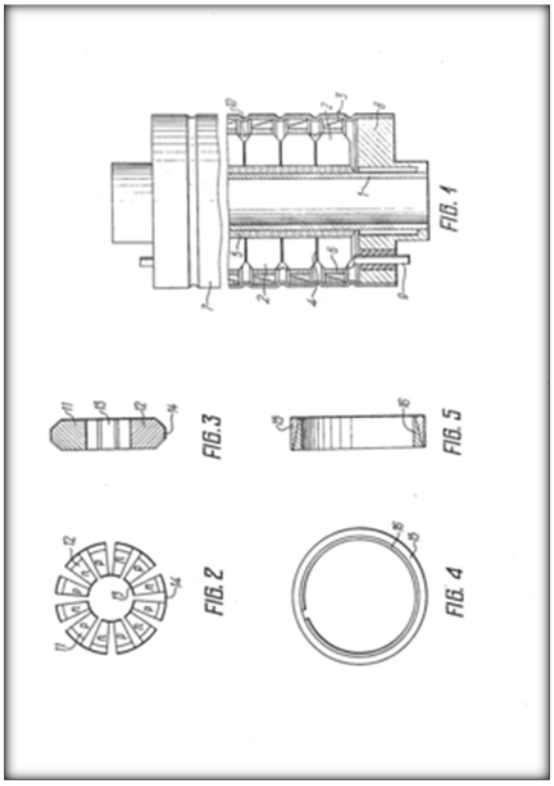

Figure 20. Schematic of first tubular thermoelectric modules consists of p- type n-type semiconductors. (From [28])

3.2 Motivation of utilizing TTEG

Some major advantages come from using tubular device are:

1- increasing the contact surface:

Obviously, contacting a plane surface and a roundish surface makes a very small contact surface between the TEG and the tubular shape heat source. It causes the amount of transferred heat to reduce strikingly. The tubular device provides a complete contact surface between the heat source and the TEG

2- simplifying the installation and design implication:

Using the flat TEG with pipes requires providing extra parts such as fixtures, outer shell or changing in the shape of the heat source pipe to a rectangular duct that prevent the TEG module from movement and structural stability. It causes extra time, cost and effort for engineers to implement a TEG in such systems. The tubular TEG would be compatible in shape and easy to install for tubular form of heat waste source.

Vehicle companies are competitively working on TEG energy recover systems. GM with the corporation of U.S. Department of Energy, conducted research on recovering wasted heat from exhausted gas. The result of 57 watts (~ 3%) of recovered energy is achieved [29]. This recovered energy can be stored in a battery, use in an electrical system, or use in main shaft. In a 22 Million dollar research, their aim is to gain 5% increase in efficiency in their future work. In fact, the Vehicle Technologies Office of Department of Energy has set the goal to increase the overall vehicle fuel economy more than 7.5 % by providing TEG technologies in vehicles until 2020. These figures show the importance of investigation in this field. Analytical studying of tubular TEG will be a good start to show how effective these systems would be. In this chapter, we offer an analytical model for tubular thermoelectric modules help for design, optimization or select proper dimension and geometry. There have been decent researches on optimization of efficiency and delivered power of flat (rectangular) TEG or

experimenting performance of tubular thermoelectric generators [30] [31] [32] [33] [34] [35].

This study looks at an analytical approach of tubular thermoelectric generator (TTEG) regardless of fabrication techniques. Tubular geometry of TEG is very useful in heat recovery from heat sources in tube shape. It enables engineers to install TEM systems on hot pipelines or tubes without disassembling, changing, or shutting off flow lines (ex: in process flow lines). In the first step, we develop an ideal model of such a device, then expand our analysis to a more realistic model, and finally compare the models.

3.3 Fabrication and Material

The special shape of the TTEG is a major challenge for the material selection and fabrication process. Commonly, material selection and fabrication process are related to operation condition of final device and demanded material properties. Needless to say, proper mechanical properties are also important for structural integrity, enduring mechanical and thermal stress, and in even tolerate of corrosion. The most common methods of thermoelectric materials preparation are [36]

1. Czochralski Method
2. Zone Melting
3. Pressing
4. Extrusion

5. Flat Cavity Crystalization

Each method has its own advantage and disadvantage. However, Andreas Schmitz and his colleagues [37] by considering the limitation of each method, fabricate tubular thermoelements by sintering (pressing) method. One of the important factors for selecting this method is eliminating material loss when compared to cutting from prepared material. *Figure 21*

Figure 21. Tubular TEG consists of four p-type n-type thermoelements PbTe (from reference [37])

Akihiro Sakai and his colleagues [38] investigate a tubular thermoelectric generator by fabricating TTEG by melt-spinning technique combined with the spark plasma sintering (SPS) process. In this work, the dimensionless figure of merit about 0.25 is achieved.

3.4 Idealistic Model of TTEG

3.4.1 Maximum Output Power:

In the first step, we start with ideal model of tubular TEG device. The main parts are consisted of a p-type and an n-type semiconductor thermoelement. These two parts are connected together with very thin ideal conductor.

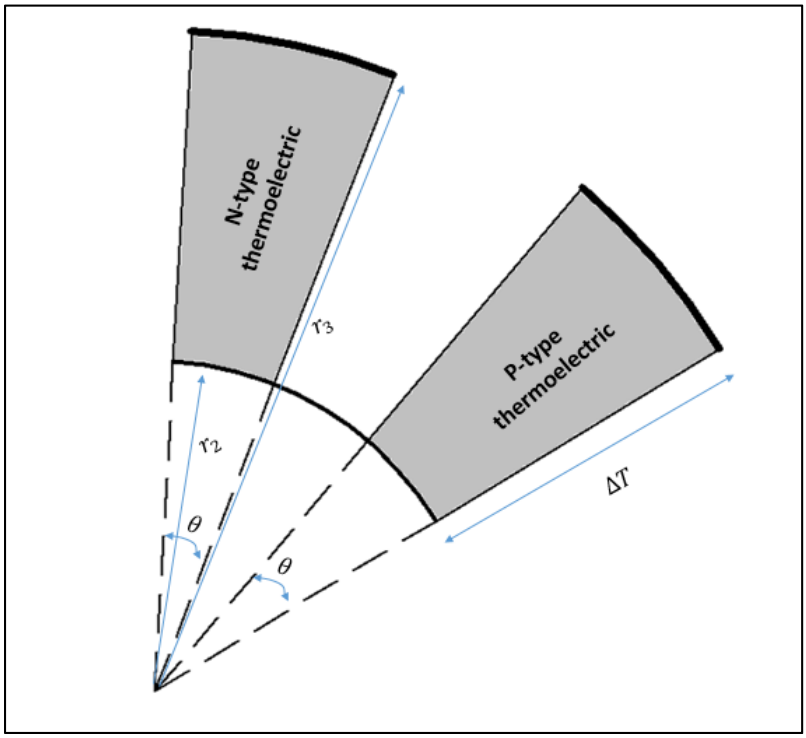

Figure 22.As illustrated in this figure, each thermoelement is a sector of cylinder wall with angle of θ and inner and outer radius of r_1 and r_2 . In this model, dimensions of two segments are assumed the same. d is length of thermoelements in perpendicular direction and thickness is r_2 - r_1 .

It can be seen that thermoelements are sectors of cylinder with the same angle measure. In the ideal case, we neglect the electrical contact resistance between conductor and elements and assume perfect contact is made. *Figure 22* Therefore, the max-generated power by this thermoelements should be

$$P_{max} = \frac{V^2}{4R}, \qquad \text{eq. (3-1)}$$

where V is electric potential of TEG, R is internal resistance of TEG= $R_p + R_n = 2R_0$ and R_0 is resistance of each thermoelement in radial direction.

Therefore

$$P_{max} = \frac{(2\,\alpha\,\Delta T)^2}{8\,R_0}, \qquad \text{eq. (3-2)}$$

where α is the seebeck coefficent and ΔT is the temperature difference of the hot and cold side.

By finding the resistance of a very small section of thermoelements and getting integral on all domain, R_0 the electrical resistivity of a cylinder section will be

$$R_0 = \int_{r_1}^{r_2} \frac{\rho\, dr}{r\theta d} = \frac{\rho}{\theta d} \int_{r_1}^{r_2} \frac{dr}{r} = \frac{\rho}{\theta d} \ln\left(\frac{r_2}{r_1}\right), \qquad \text{eq. (3-3)}$$

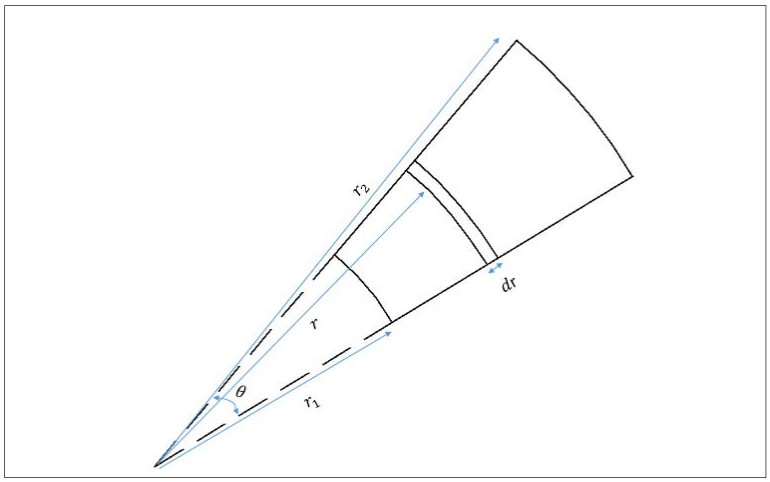

Figure 23. A section of the tubular resistor

where ρ is electrical resistivity, θ is angle measure of the section and d is thickness. *Figure 23.*

By using eq. (3-2) and eq. (3-3)

$$P_{max} = \frac{\alpha^2 \Delta T^2 \theta \, d}{2 \, \rho \ln\left(\frac{r_2}{r_1}\right)} . \qquad \text{eq. (3-4)}$$

Deriving eq. (3-1) to eq. (3-4) is under the condition that two thermoelements have the same thermal and electrical properties and geometrical features.

As *Figure 24* shows, the constant inner radius of TEG, increasing in thermoelectric material in radial direction, results in decreasing maximum output power of TEG. This trend can be attributed to the mild temperature gradient in radial direction in thermoelements. Besides, the important effect of electrical resistance will be increased when the material is accumulated in a radial direction. Therefore, less generated power is expected due to these factors.

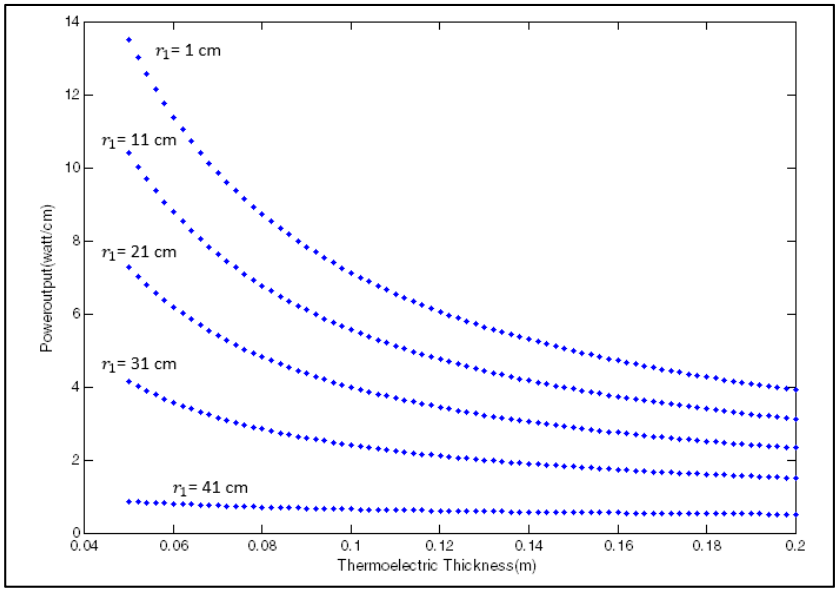

Figure 24. Shows idealistic trend of decreasing maximum delivered power to external load due to increasing in thickness of TTEG. This graph is prepared based on Bi_2Te_3 properties with $\Delta T = 150$ and $\theta = \pi$

3.4.2 Efficiency of TTEG

The most important qualitative factor, which is also important in selection and designing TEG, is considering the efficiency of the energy conversion of the device. The efficiency η is defined as

$$\eta = \frac{P}{q}, \qquad \text{eq. (3-5)}$$

where p is output-generated energy to the load and q is input heat to the hot side of the device to remain at T_h.

Specifically, generated power in the load is

$$P = R_L\, I^2. \qquad \text{eq. (3-6)}$$

To find q the heat flow in the hot side of TEG should be investigated. There are 3 main effects which are involved in the heat flow in the hot junction:

1. q_1 Generated Joule heating is a mechanism to heat up in the thermoelement. Half of this heat goes to the hot junction and half of that goes to the cold junction. Because the system loses energy with this mechanism, the sign of this term is negative. So:

$$q_1 = -\frac{1}{2}\left(R_n + R_p\right) I^2 = -R_0\, I^2. \qquad \text{eq. (3-7)}$$

2. q_2 Absorbed heat due to the flow of the current (Peltier effect) in the hot side is

$$q_2 = \left(\alpha_p - \alpha_n\right) I\, T_h = 2\,\alpha\, I\, T_h\,. \qquad \text{eq. (3-8)}$$

3. q_3 Heat flow conducted away from the hot side to the cold side by thermal conduction.

$$q_3 = \frac{\theta\, k\, d}{\ln\left({}^{r_2}/_{r_1}\right)}\,\Delta T. \qquad \text{eq. (3-9)}$$

so, total input heat which is required at the hot side of the device to remain at T_h is

$$q = q_1 + q_2 + q_3\,. \qquad \text{eq. (3-10)}$$

From eq. (3-7), eq. (3-8), eq. (3-9) and eq. (3-10)

$$q = 2\,\alpha\, I\, T_h + \frac{\theta\, k\, d}{\ln(\frac{r_2}{r_1})}\,\Delta T - R_0\, I^2, \qquad \text{eq. (3-11)}$$

and

$$I = \frac{V}{R} = \frac{2\,\alpha\,\Delta T}{4\,R_0} = \frac{1}{2}\,\frac{\alpha\,\Delta T}{R_0}. \qquad \text{eq. (3-12)}$$

From eq. (3-6), eq. (3-11) and eq. (3-12), the efficiency is

$$\eta = \frac{\Delta T}{T_h}\left[\frac{1}{2-\frac{1}{4}\frac{\Delta T}{T_h}+\frac{2}{Z\,T_h}}\right]. \qquad \text{eq. (3-12)}$$

This equation and *Figure 25* clearly show that in the ideal device, conversion efficiency only depends on temperature and figure of merit (Z) and it is independent of the dimension of TEG. Figure of merit is a thermoelectrical property of every material and is defined as

$$\mathrm{Z} = \frac{\alpha^2}{\rho\,\mathrm{k}}.$$

Because the Figure of Merit changes with temperature, to have a more meaningful index dimensionless figure of merit ZT is offered. It is worth mentioning again that the above equations are derived with the assumption of the ideal condition, by considering the homogeneous material, $\alpha_p = -\alpha_n$ and $\rho_p = \rho_n$, but in situations when we can neglect the waste energy in contact points (e.g. when the thermoelements' lengths are relatively long), the equations are valid and utilizable with an acceptable range of error.

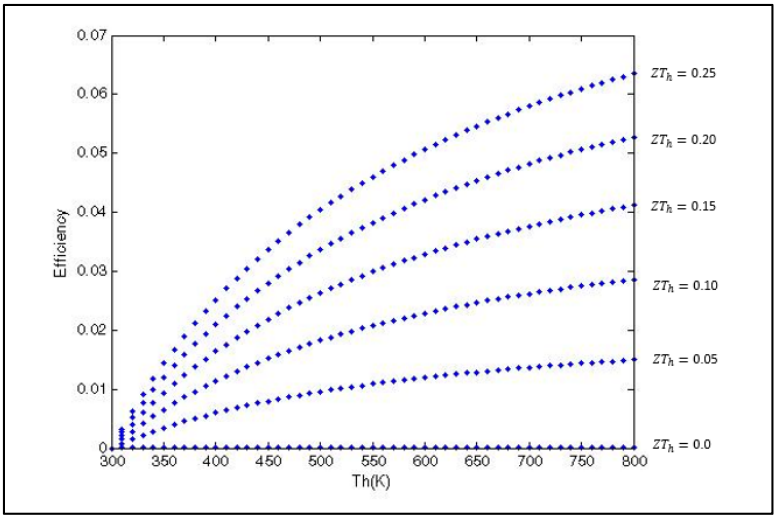

Figure 25. This figure is prepared based on $Bi_2\,Te_3$ properties in when$T_c = 300$ and $\theta = \pi$. Increasing temperature in hot junction, improved the efficiency of TTEG. Besides, increasing in Figure of Merit (ZT_h) has the same effect on efficiency as well.

3.5 Realistic Model

Like any other physical system, in the case of using TEG, due to irreversibilities such as electrical contact resistivity and thermal resistivity of contact plates, the governing equations should be re-derived, and the effect of irreversibility should be involved. Then, by investigating the effects of different variables on output power, a desirable design is achievable.

Figure 26 shows a realistic model of the TTEG that consists of two layers of contact plates, which protect thermoelectric materials from mechanical damage or chemical reaction to transfer heat properly to the hot junction.

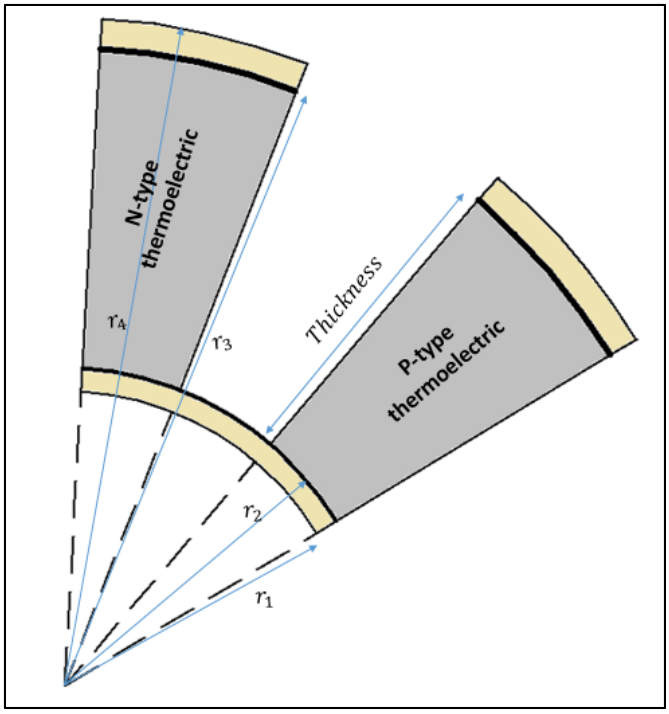

Figure 26. Thermoelectric materials are sandwiched between high thermal conductive contact plates. Temperature difference between the hot and the cold contact plates is ΔT_0. Temperature difference hot and cold junction of thermoelements is ΔT.

Contact plates are high thermal conductive, electrically insulator plates that attached to TEG to transfer heat properly to the hot junction and protect it from mechanical, chemical, and electrical damage. By considering that transferred heat is

$$\dot{Q} = 2\pi kd \frac{\Delta T}{ln(\frac{r_2}{r_1})}, \qquad \text{eq. (3-13)}$$

and Thermal resistance is

$$\lambda = R_h = \frac{\Delta T}{\dot{Q}} = \frac{\ln(\frac{r_2}{r_1})}{2\pi kd}. \qquad \text{eq. (3-14)}$$

3.5.1 Thermal-Electrical Analogy Approach:

Because of the composite layers of material in this model, for better understanding of the governing equations we use the analogy of heat flux in solids and electric current in resistors. *Figure 27*

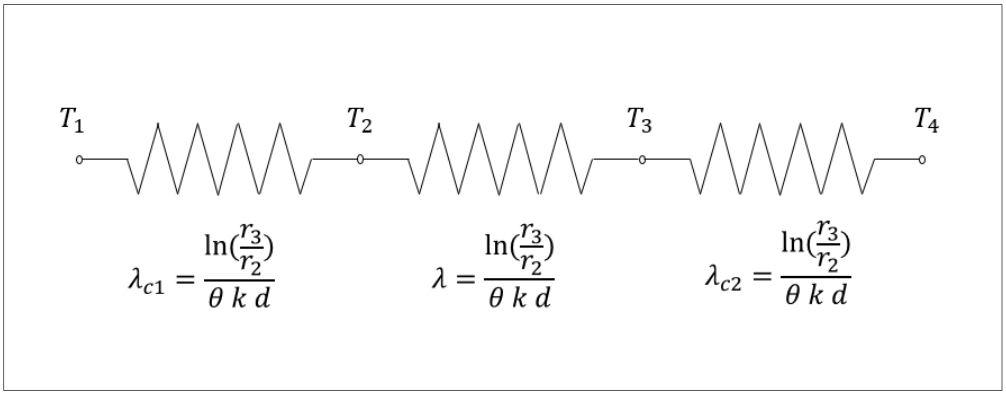

Figure 27. Thermal-electrical analogy of heat transfer in TTEG. λ_{c1} and λ_{c2} are thermal resistance of inner contact surface and outer contact surface.

We start with defining temperatures. It means

$$\begin{cases} \Delta T_0 = T_4 - T_1 \\ \Delta T = T_3 - T_2 \end{cases}. \qquad \text{eq. (3-15)}$$

Then by considering the constant rate of heat transfer,

$$\frac{\Delta T}{\lambda} = \frac{\Delta T_0}{\lambda_{c1} + \lambda + \lambda_{c2}}. \qquad \text{eq. (3-16)}$$

Using eq. (3-14), eq. (3-15) and eq. (3-16), after some steps and simplification, the temperature difference of the hot junction and cold junction is

$$\Delta T = \frac{\Delta T_0}{\left(-1 + ln\left(\frac{r_4}{r_1}\right) \Big/ ln\left(\frac{r_3}{r_2}\right)\right) r + 1}, \qquad \text{eq. (3-17)}$$

where $r = \frac{k}{k_c}$. With a proper length along z direction, temperature distribution is only along the radial direction. Neglecting thermal resistance, due to contact between thermoelements and contacting surface has been eliminated from the model, by referring to experimental results offered by [39], which confirmed the negligible amount of that with respect to other existing thermal resistance in TTEG. The main source of irreversibility with a striking effect on output is electrical contacting resistance between semiconductor thermoelements and the metallic conductor. Contacting electrical resistance is related to fabrication quality, surface roughness, and materials, so surface resistance will be

$$R_c = \frac{2\,\rho_c}{r\,\theta\,d}, \qquad \text{eq. (3-18)}$$

where, ρ_c is electrical contact resistivity, $\Omega\,.\,m^2$

Total series electrical resistance may be expressed as

$$\text{R= } 2R_0 + R_{c1} + R_{c2}. \qquad \text{eq. (3-19)}$$

Using eq. (3-3), eq. (3-18) and eq. (3-19),

$$R = \frac{2\,\rho}{\theta\,d}\left[ln\left(\frac{r_3}{r_2}\right) + n\left(\frac{1}{r_2} + \frac{1}{r_3}\right)\right], \qquad \text{eq. (3-20)}$$

where n is the electrical resistivity ratio and defined as

$$n = \frac{\rho_c}{\rho}\,.$$

3.5.2 Maximum Power and Efficiency:

By substituting eq. (3-4), eq. (3-17), eq. (3-20)

$$P_{Real} = \left(\frac{\alpha^2\,\theta\,d}{2\,\rho}\right)\frac{\Delta T_0^2}{\left[\left(-1+ln\left(\frac{r_4}{r_1}\right)/ln\left(\frac{r_3}{r_2}\right)\right)r+1\right]^2\left[\ln\left(\frac{r_3}{r_2}\right)+n\left(\frac{1}{r_2}+\frac{1}{r_3}\right)\right]}. \quad \text{eq. (3-21)}$$

This equation relates the maximum output power of a TEG unit delivered to external load to its geometrical variables and thermo-electrical properties.

From the eq. (3-20), we can see that in addition to geometry parameters, the thermal conductivity ratio (r) and relative contact resistivity (n) are involved in output power. Comparison between Figure 23 and Figure 28 shows that a realistic device has a limitation on maximum power output. In this case maximum output power occurs around 0.1 m of TEG length.

To check the performance and capability of a realistic TEG with respect to the ideal device, to generate power with the same dimensions, temperature difference and conditions, use eq. (3-4) and eq. (3- 20), where the rational efficiency (or second-law efficiency) will be defined as $\eta_r = (P_{Real}/P_{max})$ and given by

$$\frac{P_{Real}}{P_{max}} = \frac{\ln\left(\frac{r_3}{r_2}\right)}{\left[\left(-1+\frac{\ln\left(\frac{r_4}{r_1}\right)}{\ln\left(\frac{r_3}{r_2}\right)}\right)r+1\right]^2\left[\ln\left(\frac{r_3}{r_2}\right)+n\left(\frac{1}{r_2}+\frac{1}{r_3}\right)\right]}. \quad \text{eq. (3-22)}$$

Figure 29 which is correspondent to eq. (3-22) shows that by increasing device length, the realistic device performance will approach the ideal device performance, and

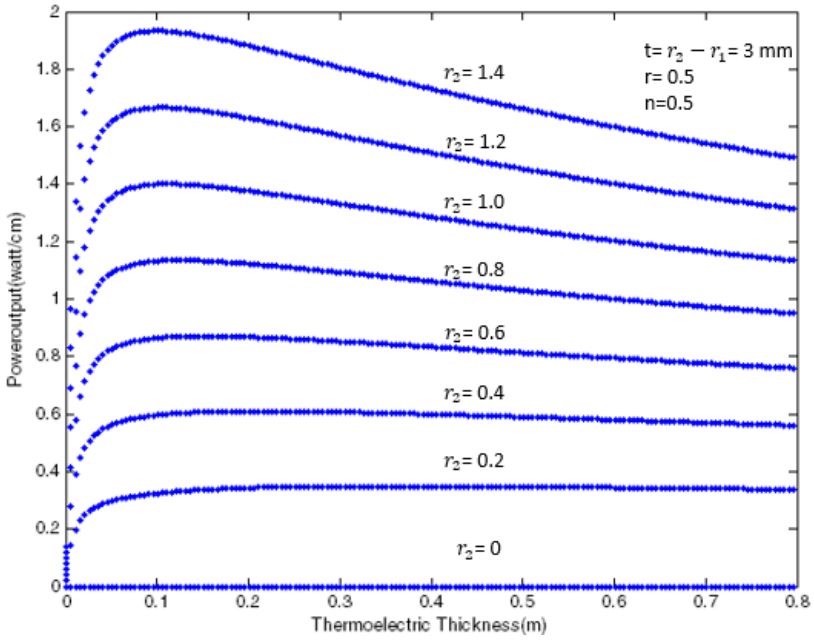

Figure 28. Power output per unit length (cm) of TTEG. Plot (a) is prepared based on $Bi_2\,Te_3$ properties when $\Delta T = 150$, $\theta = \pi$. Trends with different inner radius of the thermoelements show a maximum in output power in a certain thermoelement thickness

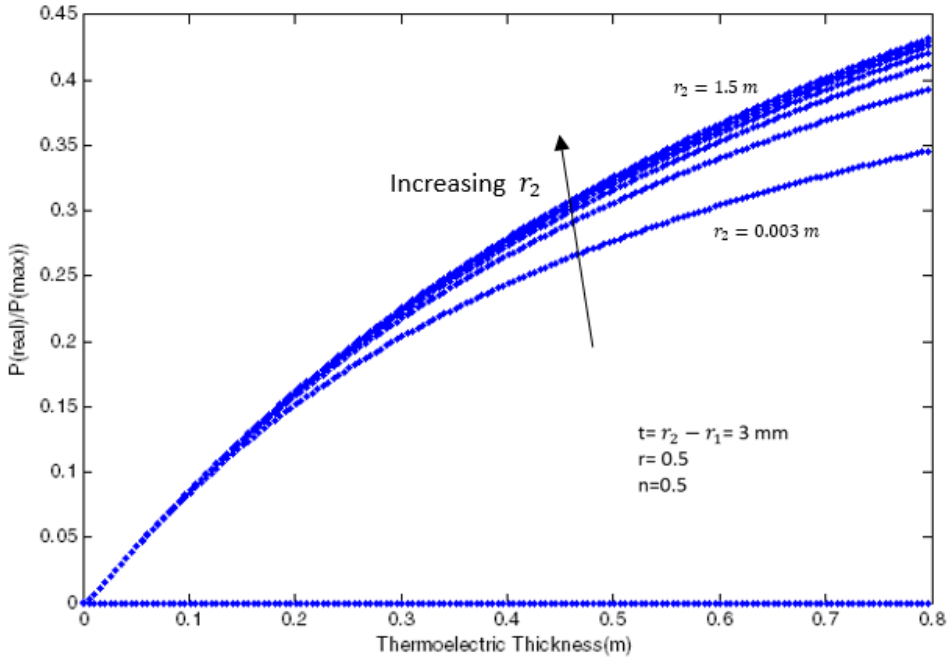

Figure 29. This figure shows effect of contact resistivity and thermal resistivity of contact plates on rational efficiency of TTEG. In this case, around maximum output power, rational efficiency of 10% is achieved

it is clearly comprehensible that below a certain amount, changing in $\frac{P_{Real}}{P_{max}}$ is not sensitive with respect to r_2, which in this case is about 0.2 m.

3.5.3 Comparison of Maximum Output Power of TEG and TTEG:

Figure 30 illustrates comparison between the results of the realistic model of TTEG and the model offered by [33] for flat TEG. With the same thermoelectric variables, thermoelement thickness and contact surface, maximum generated power in TTEG is over the TEG, particularly in optimized thickness and greater.

One of the effective factors in output power of the realistic device is the ratio of $r=\frac{k}{k_c}$. If r=0, $\Delta T = \Delta T_o$ and maximum output is achievable. Increasing r means, the thermal conductivity of thermoelectric material is increasing. It results in more sinking heat in cold junction and less power delivery to the output load. The result is describes in *Figure 31.*

Contact resistance is definitely considered as a source of irreversibility, and it is expected to reduce the efficiency of devices. Obviously, the ideal situation is where the $n = \frac{\rho_c}{\rho}$ = 0 and the contact resistance does not exist, so the delivered power is equal to the ideal device. As it is illustrated in *Figure 32*, increasing n results in decreasing delivered power to the external load.

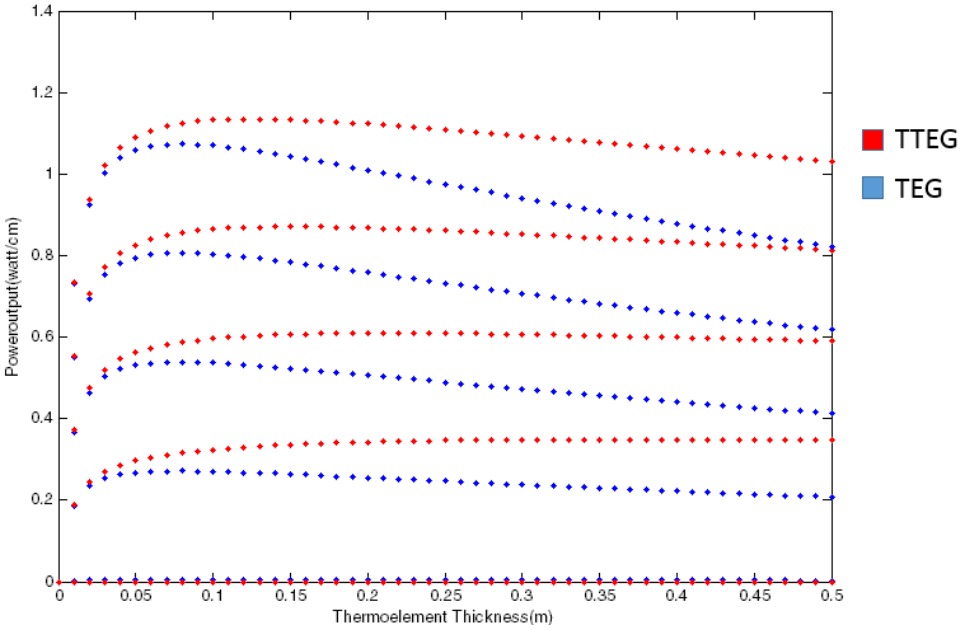

Figure 30. Comparison of power output between TTEG and flat TEG

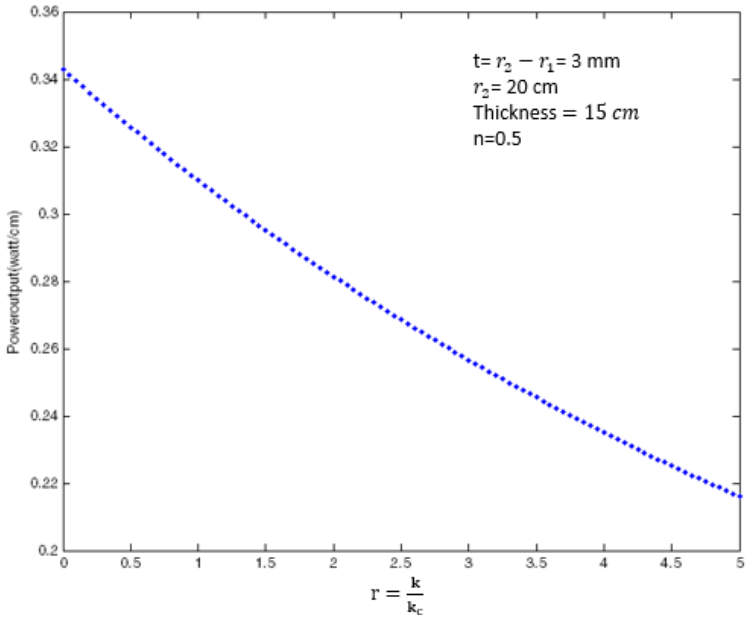

Figure 31. shows the effect of relative thermal conductivity

3.5.4 Manufacturing Quality Factor:

By development of a realistic model, it is learned that the output power and the efficiency of TTEG devices are affected by contact factors. *Figure 29* and *Figure 30* clearly showed how these contact factors r and n have striking effects on output power. Precise selection of materials and quality of fabrication for making high-quality contact surfaces are so important. Manufacturing Quality Factor (MQF) has been defined as

$$P_{Real} = F.\ P_{max}\ , \qquad \text{eq. (3-23)}$$

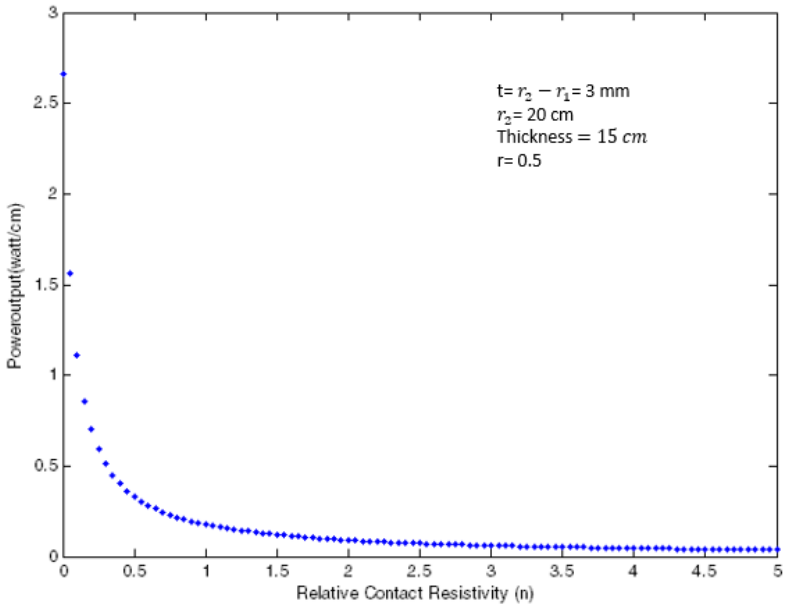

Figure 32. Shows the effect of reletive contace resistivity

where F is Manufacturing Quality Factor. By comparing eq. (3-22) and eq. (3-23), we comprehend that second-law efficiency and MQF are different representations of a unique concept. In addition to n and r, thermoelement length, $r_3 - r_2$, and contact plate thickness, $r_2 - r_1$, affect MQF.

3.6 Conclusion

In this work, the focus has been on offering simple analytical model of ideal and realistic tubular thermoelectric generators that explain the dependency of maximum delivered power to external load based on geometry variables and bulk thermoelectrical properties. The basis of this work is the ideal model, which is in good agreement with the analytical model of flat rectangular TEG in maximum output power and related efficiency.

This model indicates how the quality of fabrications would be important in efficiency and performance of TTEG, which can be increasingly improved by reducing relative contact resistivity (n) and relative thermal conductance. However, this model predicts that maximum output power usually comes with less conversion efficiency. Selection between high output power and a high efficiency coefficient should be a tradeoff between considering other variables such as the price of the provided heat source. Generally the purpose of implementing TTEG is recovering useless and out of account heat sources. Therefore, the cost-per-watt of this energy is expected to be very low, and the efficiency of the system is less important than the amount of output power.

References

[1] A. McCrone , E. Usher, V. Sonntag-O'Brien, U. Moslener and C. Grüning, "Global Trends in Renewable Energy Investment 2012," Frankfurt School - UNEP Collaborating Centre for Climate & Sustainable Energy Finance, 2012.

[2] A. Simon and R. Belles, "Estimated Energy Use in 2012," Lawrence Livermore National Laboratory, 2012.

[3] "Levelized Cost and Levelized Avoided Cost of New Generation Resources in the Annual Energy Outlook 2015," U.S. Department of Energy, 2015.

[4] "Thermoelectric Energy Harvesting 2014-2024: Devices, Applications, Opportunities," ReportLinker, 2015.

[5] D. Rowe, "Chapter1," in *Thermoelectrics Handbook Macro to Nano*, CRC Press, 2005.

[6] G. J. Synder, "Thermoelectric Power Generation: Efficiency and Compability," in *Thermoelectrics Handbook Macro to Nano*, CRC Press, 2005, p. Chapter 9.

[7] M. S. El-Genk and H. H. Saber, "Modeling and Optimization of Segmented Thermoelectric Generators for Terrestrial and Space Applications," in *Thermoelectrics Handbook, Macro to Nano*, CRC Press, 2006.

[8] H. J. Goldsmid, Introduction to thermoelectricity, Springer, 2010.

[9] I. Abram Fedorovich, Semiconductor thermoelements, and Thermoelectric cooling, London.

[10] R. Venkatasubramanian, E. Siivola, T. Colpitts and B. O' Quinn, "Thin-film Thermoelectric Devices With High Room-Temperature Figures of Merit," *Nature,* vol. 413(6856), p. p.597, 2011.

[11] V. H. Nguyen, M. C. Nguyen, H.V. Nguyen, J. Saint-Martin and P. Dollfus, "Enhanced Thermoelectric Figure of Merit in Vertical Graphene Junctions," *Appl. Phys. Lett,* 2014.

[12] K. Biswas, J. He, I. Blum, C.I. Wu, T. Hogan, D. Seidman, V. Dravid and M. Kanatzidis, "High-Performance Bulk Thermoelectrics With All-Scale Hierarchical Architectures," *Nature,* p. 414–418, 2012.

[13] I. Thomas and G. P. Srivastava, "Detailed Calculation of the Thermoelectric Figure of Merit in an N-Doped SiGe Alloy," *hysical Review B,* 2012.

[14] V. Zaitsev, M. Fedorov, I. Eremin and E. Gurieva, "Thermoelectrics on the Base of Solid Solutions of Mg2BIV Compounds," in *Thermoelectrics Handbook, Macro to Nano*, CRC Press, 2006.

[15] H.-T. Lin, Y. Katoh and J. Matyas, "The American Ceramic Society's 38th International Conference on Advanced Ceramics and Composites," in *Ceramic Materials for Energy Applications*, Florida, 2014.

[16] L.-D. Zhao, S.-H. Lo, Y. Zhang, H. Sun, G. Tan, C. Uher, C. Wolverton, V. P. Dravid and . M. G. Kanatzidis, "Ultralow Thermal Conductivity and High Thermoelectric Figure of Merit in SnSe Crystals," *Nature,* vol. 508, pp. 373-377, 2014.

[17] C. A. Gould, N. Y. A. Shammas, S. Grainger and I. Taylor, "Thermoelectric Power Generation:

Properties, Application and Novel TCAD Simulation," in *Power Electronics and Applications*, 2011.

[18] H. G. Arrendale and S. O. Ahlbrandt, "Thermoelectric Method and Apparatus for Charging Superconducting Magnets". U.S. Patent US5565763 A, 15 Oct 1996.

[19] M. Ono and T. Kuriyama, "Development of a Superconducting Magnet Excited with Thermoelectric Conversion Element for Quasi-Persistent Mode," *IEEE TRANSACTIONS ON APPLIED SUPERCONDUCTIVITY,* vol. 12, 2002.

[20] H.L. TSAI and J.M. LIN, "Model Building and Simulation of Thermoelectric Module Using Matlab/Simulink," *Journal of ELECTRONIC MATERIALS,* vol. 39, 2010.

[21] L. Chen, J. Gong, F. Sun and C. Wu, "Effect of Heat Transfer on the Performance of Thermoelectric Generators," *International Journal of Thermal Sciences,* vol. 41, no. 1, p. 95–99, 2002.

[22] J. Chávez, J. Ortega , J. Salazar, A. Turó and . M. Garcia, "SPICE Model of Thermoelectric Elements Including Thermal Effects," in *Instrumentation and Measurement Technology Conference, 2000. IMTC 2000*, Baltimore, 2000.

[23] Y. A. Cengel and M. A. Boles, Thermodynamics : An Engineering Approach, McGraw-Hill Higher Education, 2006.

[24] Y. A. Cengel, Heat Transfer: A Practical Approach, Mcgraw-Hill , 2002.

[25] M. Ono, T. Kuriyama, J. Ueda and T. Okamura, "Basic study of high Tc superconducting magnet excited by thermoelectromotive force," *Cryogenics journal,* vol. 43, p. 571–574,

2003.

[26] "Magnetic Phenomena," American Magnetics Inc, 17 March 2016. [Online]. Available: http://www.americanmagnetics.com/magnetp.php.

[27] W. T. B. de Sousa, A. Polasek, F. A. Silva, R. Dias, A. R. Jurelo and R. de Andrade, "Simulations and Tests of MCP-BSCCO-2212 Superconducting Fault Current Limiters," *IEEE Transactions on Applied Superconductivity,* vol. 22, 2012.

[28] M. A. Markman, L. M. Simanovsky, I. R. Jurkevich, N. V. Kolomoets, V. T. Kamensky, I. M. Matskov and S. I. Maximov, "Tubular thermoelectric module". U.S. Patent US 4056406 A, 1 Nov 1975.

[29] G. P. Meisner, "Skuttxerudite Thermoelectric Generator For Automotive Waste Heat Recovery," U.S. Department of Energy, 2010.

[30] D. Rowe and G. Min, "Evaluation of thermoelectric modules for power generation," *Journal of Power Sources,* pp. 193-198, 1998..

[31] D. Rowe and G. Min, "Evaluation of thermoelectric modules for power generation," *J Power Sources,* vol. 73, p. 193–198, 1998.

[32] Jincan Chen and Chih Wu, "Analysis on the Performance of a Thermoelectric Generator," *Journal of Energy Resources Technology,* vol. 122(2), p. 61, 2000.

[33] D. Rowe, "Peltier Devices as Generators," in *CRC Handbook of Thermoelectrics*, CRC Press, 1995, pp. 479-489.

[34] L. Chen, F. Meng and S. Fengrui, "Internal and external simultaneous optimization of an irreversible thermoelectric generator for maximum power output," *International Journal of Low-Carbon Technologies ,* p. 188–196, 2013.

[35] C. Wu, "Analysis of Waste-Heat Thermoelectric Power Generators," *Applied Thermal Engineering,* vol. 16, p. 63–69, 1996.

[36] Maniakin, Sergei M , Belov, Yury M , Morgunov, Igor V, "Review of Methods of Thermoelectric Material Mass Production," in *Thermoelectric Hand Book, Macro to Nano*, CRC Press, 2006.

[37] A. SCHMITZ, C. STIEWE and E. MULLER, "Preparation of Ring-Shaped Thermoelectric Legs from PbTe Powders for Tubular Thermoelectric Modules" *Journal of ELECTRONIC MATERIALS,* vol. 42, 2013.

[38] A. SAKAI, T. KANNO, K. TAKAHASHI, H. TAMAKI, H. ADACHI and Y. YAMADA, "Enhancement in Performance of the Tubular Thermoelectric Generator (TTEG)," *Journal of ELECTRONIC MATERIALS,* vol. 42, 2013.

[39] "U.S. Department of Energy," Feb 2016. [Online]. Available: http://energy.gov/eere/vehicles/vehicle-technologies-office-waste-heat-recovery.

[40] Sakai, Akihiro ; Kanno, Tsutomu ; Takahashi, Kouhei ; Tamaki, Hiromasa ; Adachi, Hideaki ; Yamada, Yuka, "Enhancement in Performance of the Tubular Thermoelectric Generator (TTEG)," *Journal of Electronic Materials,* vol. 42(7), pp. 612-1616, 2013.

[41] R. R.Heikes, Thermoelectricity: Science and Engineering, New York: Interscience Publishers,

Inc., 1961.

[42] D. Rowe, "General Principles and Theorotical Considrations," in *Thermoelectrics Handbook: Macro to Nano*, CRC Press, 2005, pp. 1-15.

[43] M. Jaegle, "Multiphysics Simulation of Thermoelectric Systems - Modeling of Peltier-Cooling and Thermoelectric Generation," in *Proceedings of the COMSOL Conference*, Hannover, 2008.

[44] Y. A. Cengel, Heat Transfer: A Practical Approach, Mcgraw-Hill, 2002.

[45] G. Min, "Optimisation of Thermoelectric Module Geometry for 'Waste Heat' Electric Power Generation," *Journal of Power Sources,* pp. 253-259, 1992.

[46] G. P. Carver, J. J. Kopanski , D. B. Novotny , R. A. Forman, "Specific Contact Resistivity of Metal-Semiconductor Contacts-a New, Accurate Method Linked to Spreading Resistance," *IEEE Transactions on Electron Devices,* vol. 35, no. 4, pp. 489 - 497, 1988.